Phylogenetic systematics of the keratin-feeding genus *Polynoncus* Burmeister, 1876 (Coleoptera: Scarabaeoidea: Trogidae)

Vinícius da Costa-Silva [1,2,3,*], Werner P. Strümpher[4], , Patricia J. Thyssen[1], and Fernando Z. Vaz-de-Mello[2]

[1]Laboratório de Entomologia Integrativa, Departamento de Biologia Animal, Instituto de Biologia, Universidade de Campinas (UNICAMP), 13083-862, Campinas, São Paulo, Brazil

[2]Laboratório de Scarabaeoidologia, Instituto de Biociências, Universidade Federal de Mato Grosso (UFMT), 78060-900, Cuiabá, Mato Grosso, Brazil

[3]Department of Zoology and Entomology, University of Pretoria, Private Bag X20, Hatfield, 0028, South Africa

[4]Ditsong National Museum of Natural History, Department of Coleoptera, P.O. Box 413, Pretoria, 0001, South Africa

*Corresponding author. Department of Zoology and Entomology, University of Pretoria, Private Bag X20, Hatfield, 0028, South Africa. E-mail: silvavinicius92@gmail.com

Abstract

Among the five known Trogidae genera, *Polynoncus* is the only one endemic to South America. Although the systematics within Trogidae is well established, the evolutionary relationships among *Polynoncus* species remain poorly understood. Here, we conducted a phylogenetic analysis based on maximum parsimony, using the equal and implicit weighting algorithm with all characters, in TNT v.1.5 software. The assembled data matrix consisted of 98 morphological characters scored for 48 taxa. Our results corroborate the monophyletic status of *Polynoncus* and its sister-group relationship with the genus *Omorgus*, both within Omorginae. In *Polynoncus*, three main lineages were recovered: (i) clade '*pedestris*', with four species occurring mostly in the Andes; (ii) clade '*pilularius*', whose species have been most reported in the temperate zone of South America; and (iii) clade '*brevicollis*', whose species are distributed from the arid zones of Argentina and Chile to Peru, following through the Andes. This is the first species-level phylogeny presented for Trogidae.

Keywords: Omorginae, South American, Neotropical region, beetles, cladistic analysis, morphology, implied weighting

Introduction

Among the five known Trogidae MacLeay, 1819 genera (Nikolajev 2016; for an overview of the family, also see: Strümpher *et al*. 2016) *Polynoncus*Burmeister, 1876 is the only genus whose distribution is restricted to South America (Vaurie 1962, Scholtz 1990b, Costa-Silva *et al.* 2024a). This genus includes currently 38 species of small to large-bodied (~5–20 mm in length) beetles (Vaurie 1962, Scholtz 1990b, Costa-Silva *et al.* 2024a). Like other trogids, *Polynoncus* larvae and adults are classified as true keratinophagous beetles due to their ability to digest keratin, a remarkable feeding specialization that is a unique evolutionary adaptation within Scarabaeoidea (see: Hughes and Vogler 2006).

The first comprehensive morphological-based phylogenetic study within and among Trogidae genera was carried out by Scholtz (1986). The classification proposed by Scholtz (1986) restored the monophyletic status of Trogidae with two distinct lineages: the first consists of the genus *Trox*Fabricius, 1775 [which includes the subgenera *Trox* + *Phoberus*MacLeay, 1819 (the latter elevated to a genus by: Strümpher *et al*. 2016)], and the other of the genera *Omorgus*Erichson, 1847 [which includes the subgenera *Haroldomorgus*Scholtz, 1986 + (*Omorgus* + *Afromorgus*Scholtz, 1986)] and *Polynoncus* (see: Scholtz 1986: fig. 1). Furthermore, based on synapomorphies (e.g. dispersal of metatarsal setae dense and elongate antennal scape), Scholtz's (1986) phylogeny drew attention to the evolutionary relationship between *Polynoncus* and *Omorgus* (both included in the subfamily Omorginae—see: Nikolajev 2005), which has since remained stable for three decades.

The phylogenetic hypothesis that *Polynoncus* evolved from an *Omorgus*-like ancestor *c*. 117 Mya (Early Cretaceous) was later supported by studies that adopted both a morphological (Scholtz and Peck 1990, Browne *et al*. 1993) and, more recently, molecular (Strümpher *et al*. 2014) approach to the classification of the two genera. In fact, Strümpher *et al*. (2014) provided robust support for subfamily and genera relationships, showing the dated evolutionary history of each group within Trogidae, and obtained a topology like those founded by Scholtz (1986). Strümpher *et al*. (2014) also confirmed *Polynoncus* monophyly.

Although the Trogidae family has a well-established phylogenetic classification, as observed by Scholtz (1986) and Strümpher *et al*. (2014), the knowledge regarding the evolutionary relationship within *Polynoncus* remains limited and speculative. In this context, our study aims to elucidate the evolutionary relationships among *Polynoncus* species based on morphological characteristics. This is the first phylogenetic study of Trogidae at the species-level and will, therefore, be a significant contribution to the ever-expanding knowledge of the natural history and evolutionary biology of this group.

Materials and methods

Taxonomic coverage and examined material

The ingroup included all 38 valid species of *Polynoncus* (*sensu*Costa-Silva *et al*., 2024a) (Table 1). *Omorgus suberosus* (Fabricius, 1775), *Omorgusfuliginosus* (Robinson, 1941) (subgenus *Omorgus*); *Omorgus squalidus* (Olivier, 1789), *Omorgusgemmatus* (Olivier, 1789) (subgenus *Afromorgus*); *Omorgus batesi* (Harold, 1872) (subgenus *Haroldomorgus*); *Trox plicatus*Robinson, 1940, and *Troxvariolatus*Melsheimer, 1846; *Phoberus montanus* (Kolbe, 1891) and *Phoberusluridus* (Fabricius, 1781) were selected as an outgroup based on previous Trogidae phylogenetic studies conducted by Scholtz (1986) and Strümpher *et al*. (2014). The South American species of Glaresidae, *Glaresis pardoalcaidei*Martínez *et al*., 1961, was included as an outermost terminal (root); until the publication of Scholtz (1986), *Glaresis* species were seen as belonging to the family Trogidae. Furthermore, several studies confirm that there is an evolutionary relationship between Trogidae and Glaresidae, i.e. sharing the trilobed aedeagal as a plesiomorphic characteristic between extant scarabaeoids (e.g. Iablokoff-Khnzorian 1977, Scholtz 1986, 1990a, d'Hotman and Scholtz 1990, Nel and Scholtz 1990, Browne and Scholtz 1995, 1999, Pretorius and Scholtz 2001, Smith *et al*. 2006, McKenna *et al*. 2019, Ballerio *et al*. 2023, Dietz *et al*. 2023).

Table 1. List of the terminals included in the morphological phylogeny dataset, follow by the type species, gender (when available), local of repositories and geographical distribution provide by Zídek (2017), and Costa-Silva *et al.* (2024a). Abbreviations: HT = holotype; LT = lectotype; NT = neotype; Y = Yes; N = No. ** indicate the type-species of the genus or subgenus. [1] See Costa-Silva *et al.* (2024b) for more information.

Family/ Subfamily	Terminals	Types and repositories	Geographical distribution	Type examined
Ingroup				
Trogidae/ Omorginae	*Polynoncus aeger* (Guérin-Meneville, 1830)	LT (MNHN)	Neotropical	Y
	Polynoncus argentinus (Harold, 1872)	HT ♂ (MNHN)	Neotropical	Y
	Polynoncus aricensis (Gutiérrez, 1950)	HT ♂ (MZUC)	Neotropical	Y
	Polynoncus bifurcatus (Vaurie, 1962)	HT ♂ (MFNB)	Neotropical	Y
	Polynoncus brasiliensis (Vaurie, 1962)	HT ♂ (MZSP)	Neotropical	Y
	Polynoncus brevicollis (Eschscholtz, 1822)	LT (ZMUM)	Neotropical	Y
	Polynoncus bullatus (Curtis, 1844)	LT (BMNH)	Neotropical	Y
	Polynoncus burmeisteri Pittino, 1987	HT ♂ (MNHN)	Neotropical	Y
	Polynoncus chilensis (Harold, 1872)	LT ♂ (MNHN)	Neotropical	Y
	Polynoncus crypticus Diéguez, 2019	HT ♂ (MNNC)	Neotropical	Y
	Polynoncus diffluens (Vaurie, 1962)	HT ♀ (CASC)	Neotropical	Y
	Polynoncus ecuadorensis (Vaurie, 1962)	HT ♂ (ZMUC)	Neotropical	Y
	Polynoncus erugatus Scholtz, 1990	HT ♀ (IFML)	Neotropical	Y
	Polynoncus furcillifer Pittino, 1987	HT ♂ (RPMI)	Neotropical	Y
	Polynoncus galapagoensis (Van Dyke, 1953)	HT ♀ (CASC)	Neotropical	Y
	Polynoncus gemmifer (Blanchard, 1847)	LT ♀ (MNHN)	Neotropical	Y
	Polynoncus gemmiferus (Blanchard, 1847)	LT ♀ (MNHN)	Neotropical	Y
	Polynoncus gemmingeri (Harold, 1872)	LT (MNHN)	Neotropical	Y
	Polynoncus gibberosus Scholtz, 1990	HT ♂ (USNM)	Neotropical	Y
	Polynoncus gordoni (Steiner, 1981)	HT ♂ (USNM)	Neotropical	Y
	Polynoncus hemisphaericus (Burmeister, 1876)	LT (MACN)	Neotropical	Y
	Polynoncus juglans (Ratcliffe, 1978)	HT ♂ (INPA)	Neotropical	Y
	Polynoncus longitarsis (Harold, 1872)	HT (MNHN)	Neotropical	Y
	Polynoncus mirabilis Pittino, 1987	HT ♂ (RPMI)	Neotropical	Y
	Polynoncus neuquen (Vaurie, 1962)	HT ♂ (MFNB)	Neotropical	Y
	Polynoncus pampeanus (Burmeister, 1876)	LT (MACN)	Neotropical	Y
	Polynoncus parafurcatus Pittino, 1987	HT ♂ (MNHN)	Neotropical	Y

	Polynoncus patagonicus (Blanchard, 1847)	LT ♀ (MNHN)	Neotropical	Y
	Polynoncus patriciae Pittino, 1987	HT ♂ (RPMI)	Neotropical	Y
	Polynoncus pedestris (Harold, 1872) **	LT ♀ (MNHN)	Neotropical	Y
	Polynoncus peruanus (Erichson, 1847)	LT ♂ (MFNB)	Neotropical	Y
	Polynoncus pilularius (Germar, 1823)	LT (MNHN)	Neotropical	Y
	Polynoncus pittinoi Costa-Silva and Diéguez, 2020	HT ♂ (MACN)	Neotropical	Y
	Polynoncus pseudogemmifer Costa-Silva *et al.*, 2024	HT ♂ (MNHN)	Neotropical	Y
	Polynoncus sallei (Harold, 1872)	HT ♂ (MNHN)	Neotropical	Y
	Polynoncus seymourensis (Mutchler, 1925)	HT (AMNH)	Neotropical	Y
	Polynoncus tenebrosus (Harold, 1872)	HT (MNHN)	Neotropical	Y
	Polynoncus vazdemelloi Huchet and Costa-Silva, 2018	HT ♂ (CEMT)	Neotropical	Y
	Outgroup			
	Omorgus (*O.*) *suberosus* (Fabricius, 1775) **	NT ♂ (NHMUK)[1]	Widespread	Y
	Omorgus (*O.*) *fuliginosus* (Robinson, 1941)	HT (USNM)	Neartic	N
	Omorgus (*A.*) *squalidus* (Olivier, 1789) **	NT ♂ (TMSA)	Afrotropical	Y
	Omorgus (*A.*) *gemmatus* (Olivier, 1789)	None found	Afrotropical	N
	Omorgus (*H.*) *batesi* (Harold, 1872) **	HT ♂ (MNHN)	Neotropical	Y
Trogidae/ Troginae	*Trox plicatus* Robinson, 1940	HT (ANSP)	Neartic	N
	Trox variolatus Melsheimer, 1846	HT (MCZH)	Neartic	N
	Phoberus montanus (Kolbe, 1891)	LT (BMNH)	Afrotropical	Y
	Phoberus luridus (Fabricius, 1781)	LT (ZMUC)	Afrotropical	N
Glaresidae	*Glaresis pardoalcaidei* Martínez *et al*., 1961	HT ♂ (MACN)	Neotropical	Y

The specimens examined (Supporting Information, Table S1) were obtained from institutions listed alphabetically below (curators/managers collections are presented in parenthesis):

- AMNH: American Museum of Natural History, New York, NY, USA (Lee Herman).
- ANSP: Academy of Natural Sciences, Philadelphia, PA, USA (Jason Weintraub).
- CASC: California Academy of Sciences, San Francisco, CA, USA (Christopher C. Grinter).
- CEMT: Coleção Entomológica de Mato Grosso Eurides Furtado (former Seção de Entomologia, Coleção Zoológica da Universidade Federal de Mato Grosso), Cuiabá, Mato Grosso, Brazil (Fernando Z. Vaz-de-Mello).
- CJBH: Collection of Jean-Bernard Huchet [Private Collection], Bordeaux, France (Jean-Bernard Huchet).

- CJEB: Collection of Juan Enrique Barriga, Curicó, Maule, Chile (Juan Enrique Barriga).
- CMNC: Canadian Museum of Nature, Gatineau, Quebec, Canada (Robert Anderson and François Génier).
- CNC: Canadian National Collection of Insects, Ottawa, Ontario, Canada (Patrice Bouchard).
- CVMD: Collection of Víctor Manuel Diéguez [Private Collection], Peñalolén, Santiago, Chile (Víctor Manuel Diéguez).
- IADIZA: Instituto Argentino de Investigaciones de Zonas Áridas, Mendoza, Mendoza, Argentina (Gustavo Flores and Sergio Roig).
- IFML: Instituto Fundación Miguel Lillo, Tucumán, Argentina (Emília Perez).
- INPA: Instituto Nacional de Pesquisas Amazônicas, Manaus, Amazonas, Brazil (Marcio Oliveira and José Albertino).
- MACN: Museo Argentino de Ciencias Naturales 'Bernardino Rivadavia', Buenos Aires, Argentina (Pablo Mulieri).
- MCNZ: Museu de Ciências Naturais da Secretaria Estadual do Meio Ambiente e Infraestrutura do Rio Grande do Sul, Porto Alegre, Rio Grande do Sul, Brazil (Luciano Moura).
- MFNB: Museum für Naturkunde, Leibniz Institut für Evolutions und Biodiversitätsforschung, Berlin, Germany (Bernd Jaeger).
- MLPA: Museo de La Plata, La Plata, Argentina (Nora Cabrera and Adriana Marvaldi).
- MNHN: Muséum national d'Histoire naturelle, Paris, France (Olivier Montreuil and Antoine Mantilleri).
- MNNC: Museo Nacional de Historia Natural, Santiago, Chile (Mario Elgueta).
- MZSP: Museu de Zoologia da Universidade de São Paulo, São Paulo, Brazil (Sônia Casari).
- MZUC: Museo de Zoología de la Universidad de Concepción, Concepción, Chile (Myriam Angélica Ramirez).
- NHMUK: The Natural History Museum, London, United Kingdom (Maxwell Barclay and Michael Geiser).
- RPMI: Collection of Riccardo Pittino [Private Collection], Milan, Italy (Riccardo Pittino).
- TMSA: Ditsong National Museum of Natural History, Pretoria, South Africa (Werner P. Strümpher).
- USNM: United States National Museum, Washington, DC, USA (Floyd Shokley).
- ZMUC: Zoological Museum, University of Copenhagen, Copenhagen, Denmark (Alexey Solodovnikov).
- ZMUM: Zoological Museum, Moscow Lomonosov State University, Moscow, Russia (Aleksey A. Gusakov).
- ZUEC: Museum of Zoology Adão José Cardoso of the University of Campinas (UNICAMP), Campinas, São Paulo, Brazil (André Victor Lucci Freitas).

Laboratory procedures for characters evaluation

For better visualization and analysis of the morphological structures, the specimens were cleaned following the protocols of Diéguez (2008) and Costa-Silva and Diéguez (2020). In addition, some specimens of each species had their mouthparts, posterior wing, and male terminalia dissected. To relax the musculature, the specimens were submerged in warm water and detergent for 10 min.

To separate the mouthparts, precise pressure was applied with fine tweezers to the region near to the gula–labium suture and the cardo. A pin was then used to completely detach the mandibles and maxillae. Finally, with the aid of a microstyler, the joint line was cut and the labrum was detached from the clypeus. The separated mouthparts were then subjected to a 10% potassium hydroxide (KOH) solution for cleaning. After the examination, the mouthparts were placed in a microvial with glycerine and pinned to the respective dissected specimen.

The left elytron was carefully lifted using a fine tweezer and the posterior wing was removed at the tergum, keeping its joint intact. The wing was then extended, mounted on paper, and pinned below its respective specimen (see detailed protocol in: Browne and Scholtz 1994).

The genitalia and spiculum were removed through the pygidium using tweezers, and were subsequently clarified and desclerotized with 10% KOH solution (see details in: Cristóvão and Vaz-de-Mello 2020). For old specimens, we opted to totally remove the abdomen to avoid possible damage to the genitalia. The card with the glued genitalia was pinned below its respective specimen.

For the general external structures of Trogidae, we followed the terminologies proposed by Vaurie (1962), Costa-Silva *et al*. (2024a), while for the terminalia we followed the propositions of d'Hotman and Scholtz (1990). Terminologies from Browne and Scholtz (1994) and Beutel and Yavorskaya (2019) were adopted for wings and mouthparts, respectively. All photographs were taken using a Leica model m205C stereomicroscope (7.8X-160.0X) with MC190 HD image capture system.

Matrix of characters

The morphological character matrix was assembled using the web application MorphoBank v.3.0 (https://morphobank.org/index.php) (O'Leary and Kaufman 2011). Matrix assembly followed the structure proposed by Sereno (2007), which uses fundamental functional components, identified as locator, variable, character state, and qualifier, to understand and recognize an evaluated character. Coding was performed using binary and multistate characters, all of which were considered as non-additive (or non-ordered). Thus, all transformation pathways had the same evolutionary cost (one step). Non-comparable/applicable and unknown characters (or not observed) were encoded by (-) and (?), respectively, following the NEXUS formating model (Strong and Lipsbomb 1999). All character states started with the encoding '0', but this did not necessarily represent a plesiomorphic condition.

All character analysis was based on the external morphology of each taxon. Although the male and female terminalia have been exhaustively studied, only the male genitalia were coded, since the female structures, such as the gonocoxite and stylus, showed great intraspecific variation, making it difficult to determine a hypothesis of homology (d'Hotman and Scholtz 1990).

Phylogenetic analysis

Phylogenetic analyses were performed based on maximum parsimony (MP) as optimality criterion as implemented in TNT v.1.5 (Goloboff *et al*. 2008a, Goloboff and Catalano 2016). The assembled character matrix was analysed under equal weighting (EW) and implied weight (IW). The heuristic search for EW was implemented with 'Traditional Search' algorithm

(Analyse > Traditional Search), where the commands for analysis were (TNT command line given in brackets): memory tree = 1 000 000 [hold1000000], random seed = 0 [rseed = 0], number of additional sequences = 1000, tree save per replication = 100. RAS + TBR (stepwise addition) was used as the permutation algorithm of the branches. The generated trees were then collapsed to ensure that the nodes that were artificially resolved and not supported by any synapomorphy were grouped correctly, thus avoiding the generation of false topologies.

The same parameters used for the EW analysis were also used for the IW character analysis (Goloboff 1993, Goloboff *et al*. 2008b). To determine the effect of down weighting homoplasy characters and to identify the best concavity constant (*k*-value) for the IW analysis, a search was conducted using the script 'aaa.run' in TNT (Mirande 2009). The search yielded 11 *k*-values from the most parsimonious trees (MPT). Therefore, the best *k*-value was selected based on the generated subtree pruning regrafting (SPR) scores, with higher values taken to indicate better congruence.

Branch supports were estimated using relative Bremer support (RBS; Goloboff and Farris 2001) and symmetric resampling (SR; Goloboff *et al*. 2003). For RBS, different search parameters were defined according to the number of extra steps ($N = 1, 2, 3, \ldots, 10$), via TBR analysis, which was performed manually on the MPTs [sub *N* hold $N \times 2000$; bb = tbr fillonly; unique*]. At the end of the analysis, the steps Tree > Bremer Support > relative supports were performed. For the resampling method (SR), 10 000 replicates were used, specifying a change probability of 33 (as default—see: Goloboff *et al*. 2003).

The consistency index (CI), retention index (RI), number of steps (L), and a list of synapomorphies were obtained and visualized in WINCLADA v.1.00.08 (Nixon 2002). The topologies found were handled in FigTree v.1.4.3 software.

Results

Dataset

The morphological dataset comprises 98 characters scored for 48 taxa. With the exception of the terminalia (Supporting Information, Table S2), no other secondary morphological characters were observed in *Polynoncus* species [with the exception of *Polynoncuscrypticus*Diéguez, 2019 and *Polynoncusgemmiferus* (Blanchard, 1847); see: Costa-Silva *et al.* 2024a], meaning that all characters used here do not vary between the sexes. Among the binary and multistate characters there were 24 associated with the head, 59 with the thorax (comprising the hindwings, pronotum, scutellum, elytra, and legs), 14 with the male terminalia, and one with the immature stage. The list of characters and parameters (including L, CI, and RI) associated with each character are shown below.

1. Head; antennae; scape shape [L = 1, CI = 100, RI = 100]

- (0) rounded (Fig. 1C)
- (1) elongate (Fig. 1A, B)

2. Head; antennae; scape apex [L = 1, CI = 100, RI = 100]

- (0) symmetric (Fig. 1A)
- (1) asymmetric (Fig. 1B)

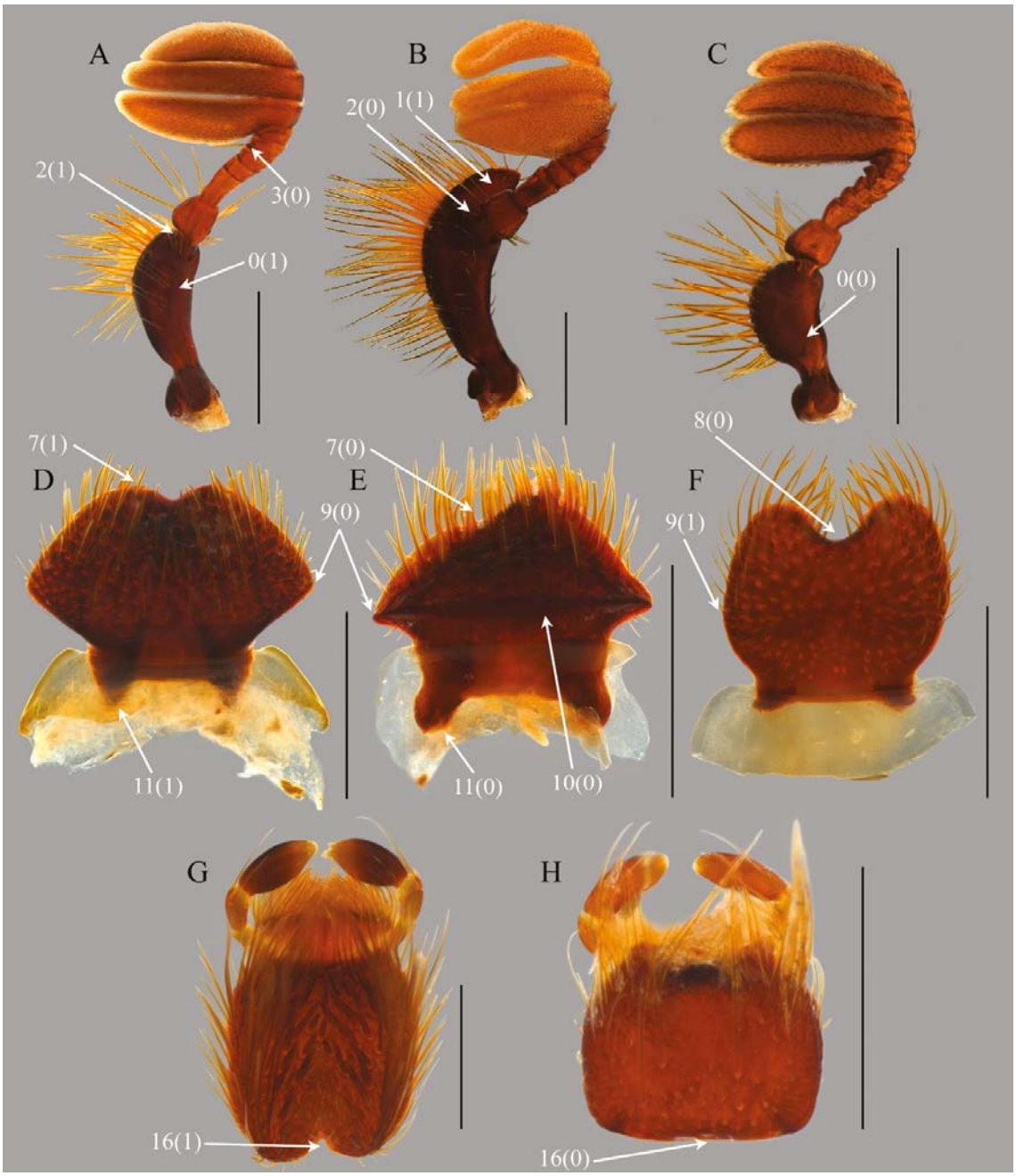

Figure 1. Characters relative of antennae and mouthparts of Trogidae: antennae of: A, *Polynoncus gemmingeri*; B, *Omorgus suberosus*; C, *Trox plicatus*. Labrum of: D, *Polynoncus juglans*; E, *Trox plicatus*; F, *Omorgus batesi* in dorsal view. Mentum of: G, *Polynoncus argentinus*; H, *Trox variolatus* in ventral view. Scale bar: 0.5 mm.

3. Head; antennae; pedicel attachment position on the scape [L = 2, CI = 50, RI = 50]

- (0) subapical (Fig. 1B)
- (1) apical (Fig. 1A, C)

4. Head; antennae; one single seta on the sixth antennomere [L = 1, CI = 100, RI = 100]

- (0) present (Fig. 1A)
- (1) absent

5. Head; ommatidium lens type (Caveney and Scholtz 1993) [L = 3, CI = 66, RI = 75]

- (0) Eucone
- (1) Duocone
- (2) Exocone

6. Head; apex of the canthus overlapping the upper margin of the eyes [L = 2, CI = 50, RI = 75]

- (0) present (Fig. 2A)
- (1) absent (Fig. 2B)

7. Head; interocular distance [L = 1, CI = 100, RI = 100]

- (0) from four to five times the length of the eyes (Fig. 2C)
- (1) twice the length of the eyes (Fig. 2D)

8. Head; mouthparts; shape of anterior labrum margin [L = 5, CI = 20, RI = 33]

- (0) asymmetric (Fig. 1E)
- (1) symmetric (Fig. 1D)

9. Head; mouthparts; anterior labrum margin with strong emargination

- (0) present* (Fig. 1F)
- (1) absent
- *state (0) is an autopomorphy of *Omorgus* (*H.*) *batesi*

10. Head; mouthparts; lateral labrum margin [L = 10, CI = 10, RI = 10]

- (0) angulate (Fig. 1D, E)
- (1) rounded (Fig. 1F)

11. Head; mouthparts; labrum with a transversal well-defined carina parallel to the posterior margin [L = 3, CI = 33, RI = 60]

- (0) present (Fig. 1E)
- (1) absent

12. Head; mouthparts; tormas apex [L = 1, CI = 100, RI = 100]

- (0) rounded (Fig. 1E)
- (1) pointed (Fig. 1D)

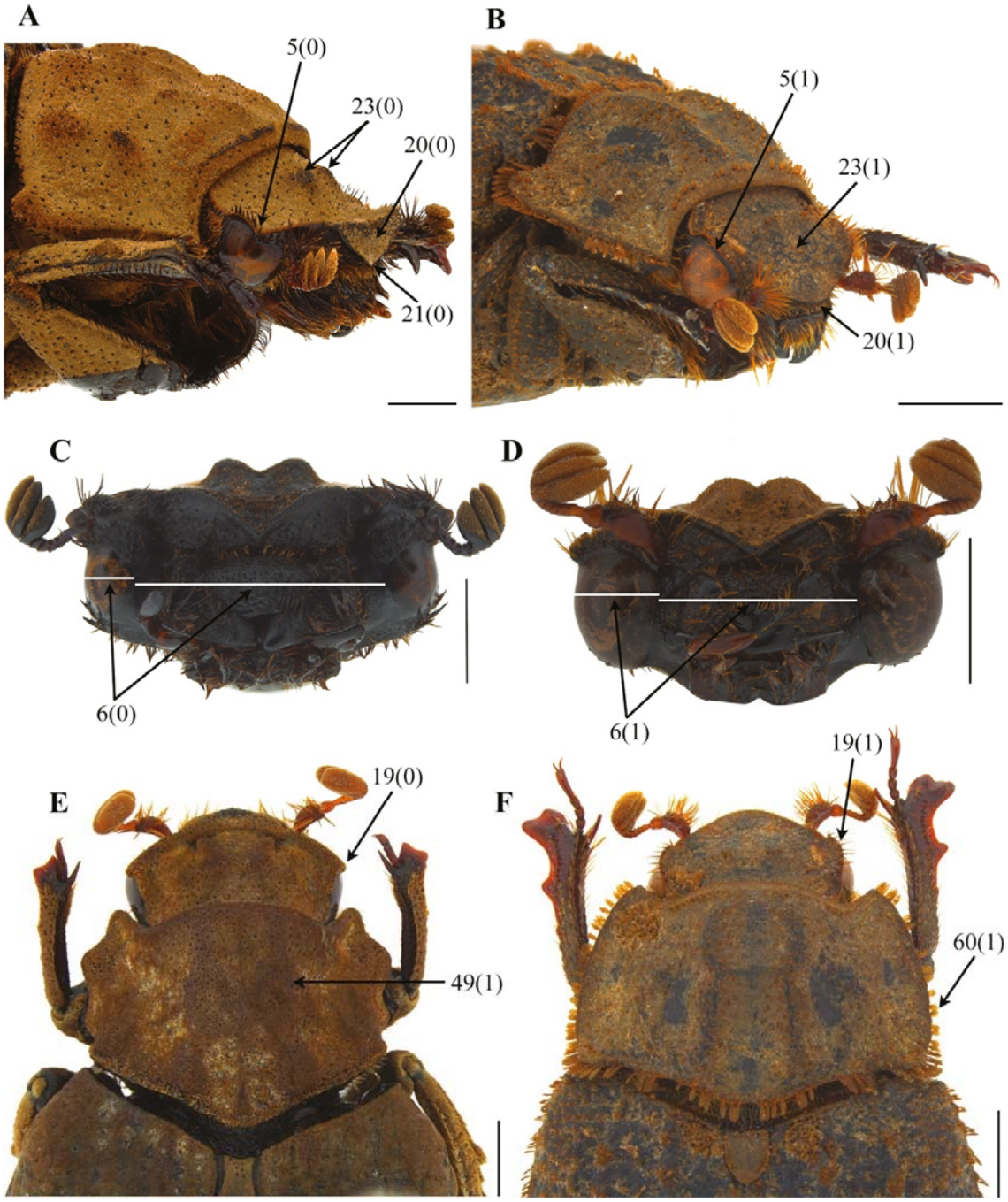

Figure 2. Characters relative of the head and pronotum of Trogidae. Fronto-lateral view of: A, *Polynoncus hemisphaericus*; B, *Trox plicatus*. Frontal view of head of : C, *Polynoncus bullatus*; D, *Polynoncusjuglans*. Dorsal view of head and pronotum of: E, *Polynoncusvazdemelloi*; F, *Trox plicatus*. Scale bar: 1 mm.

13. Head; mouthparts; fourth maxillary palpomere; sinuosity on the ventral margin near the apex [L = 2, CI = 50, RI = 90]

- (0) present (Fig. 3A)
- (1) absent

14. Head; mouthparts; lacinia shape [L = 1, CI = 100, RI = 100]

- (0) 2× longer than wide (Fig. 3A)
- (1) 4× longer than wide (Fig. 3B)

15. Head; mouthparts; second thorn at the lacinia apex

- (0) present (Fig. 3B)
- (1) absent*
- *state (1) is an autopomorphy of *Glaresis pardoalcaldei*

16. Head; mouthparts; shape of the superior thorn at the lacinia apex [L = 2, CI = 50, RI = 50]

- (0) bifurcated (Fig. 3B)
- (1) trifurcated

17. Head; mouthparts; shape of posterior mentum margin [L = 2, CI = 50, RI = 50]

- (0) straight (Fig. 3H)
- (1) bilobated (Fig. 3G)

18. Head; mouthparts; dorsal surface of the right mandible; a well-defined and raised swelling parallel to the outer margin [L = 1, CI = 100, RI = 100]

- (0) present (Fig. 3E)
- (1) absent (Fig. 3F)

19. Head; mouthparts; first tooth of the right mandible [L = 1, CI = 100, RI = 100]

- (0) well developed and rounded (Fig. 3D)
- (1) short and pointed (Fig. 3C)

20. Head; genae shape [L = 2, CI = 50, RI = 75]

- (0) angulate (Fig. 2E)
- (1) rounded (Fig. 2F)

21. Head; clypeus with apical portion downward abruptly [L = 1, CI = 100, RI = 100]

- (0) present (Fig. 2A)
- (1) absent (Fig. 2B–D)

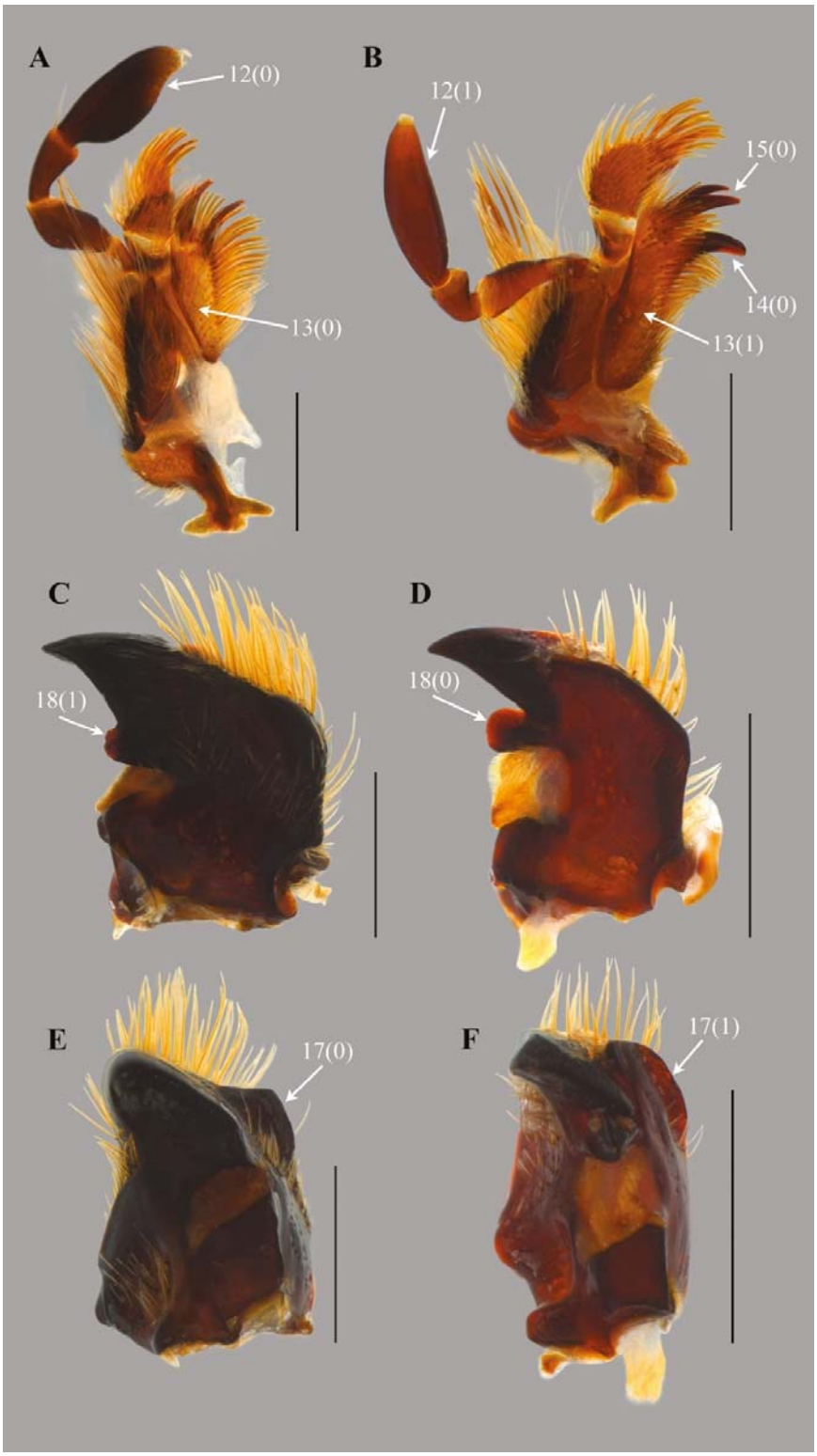

Figure 3. Characters relative of mouthparts of Trogidae. Maxila, in dorsal view, of: A, *Polynoncus argentinus*; B, *Trox luridus*. Dorsal view of right mandible of: C, *Polynoncus gemmingeri*; D, *Trox variolatus*. Lateral view of right mandible of: E, *Polynoncus gemmingeri*; F, *Trox variolatus*. Scale bar: 0.5 mm.

22. Head; shape of the downward clypeus apex [L = 3, CI = 33, RI = 0]

- (0) sharp (Fig. 2A)
- (1) rounded

23. Head; shape of the posterior clypeus margin, in dorsal view [L = 7, CI = 14, RI = 53]

- (0) truncate (Fig. 4B)
- (1) emarginate (Fig. 4A)

24. Head; two central tubercles on the front [L = 2, CI = 50, RI = 50]

- (0) present (Fig. 2A)
- (1) absent (Fig. 2B)

25. Thorax; posterior wings; visible and distinctive veins [L = 1, CI = 100, RI = 100]

- (0) present (Fig. 5A, B)
- (1) absent (Fig. 5C)

26. Thorax; posterior wings; shape [L = 3, CI = 66, RI = 83]

- (0) well developed (Fig. 5A)
- (1) reduced (Fig. 5B)
- (2) vestigial (Fig. 5C)

27. Thorax; posterior wings; sclerotization of the Sc venation [L = 1, CI = 100, RI = 100]

- (0) present (Fig. 5A)
- (1) absent

28. Thorax; posterior wings; constriction between RA3+4, RA3 and RA4 venation ('pinch') [L = 1, CI = 100, RI = 100]

- (0) present (Fig. 5A)
- (1) absent

29. Thorax; posterior wings; AA1+2 venation [L = 3, CI = 33, RI = 71]

- (0) present (Fig. 5A)
- (1) absent

30. Thorax; posterior wings; length of AA1+2 venation [L = 10, CI = 20, RI = 52]

- (0) equal of AA3+4
- (1) quarer of the length of AA3+4 (Fig. 5A)
- (2) half the length of AA3+4

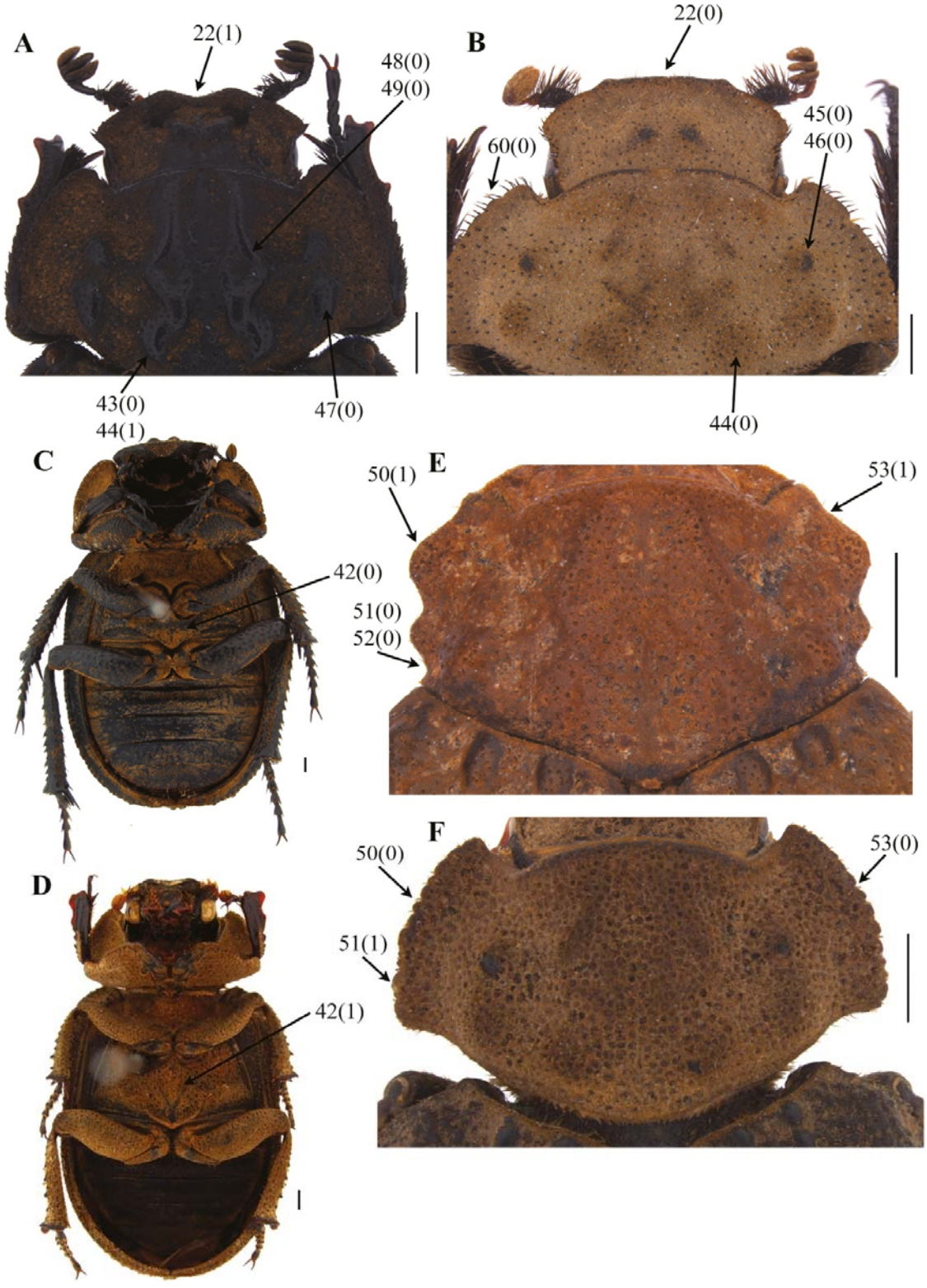

Figure 4. Characters relative of the head, pronotum and metasternum of *Polynoncus*. Dorsal view of head and pronotum in: A, *Polynoncus bullatus*; B, *Polynoncushemisphaericus*. Ventral view of body in: C, *Polynoncuspatagonicus*; D, *Polynoncusneuquen*. Dorsal view of pronotum in: E, *Polynoncus furcillifer*; F, *Polynoncusneuquen*. Scale bar: 1 mm.

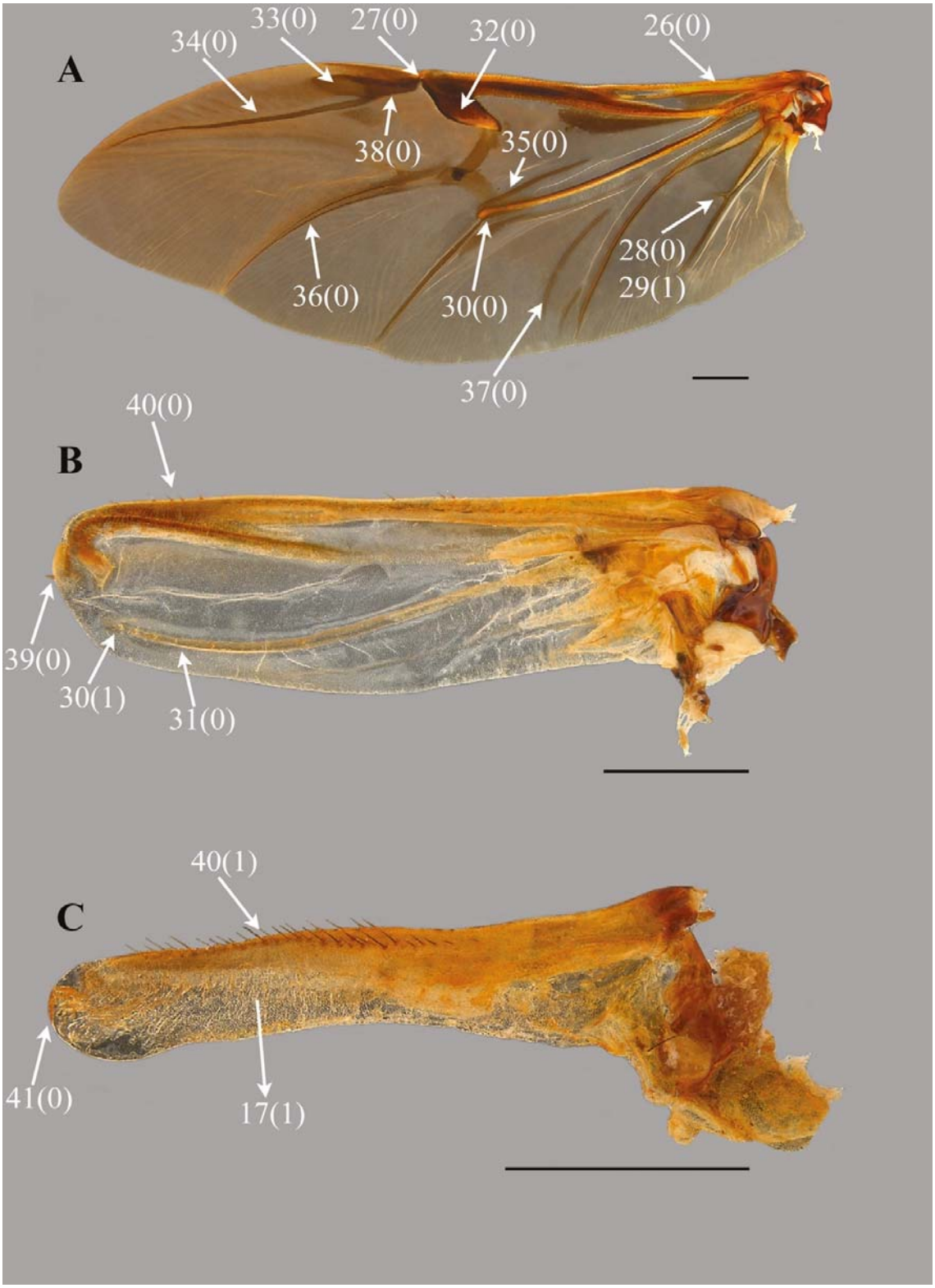

Figure 5. Characters relative of the dorsal view of left anterior wing of: A, *Polynoncus vazdemelloi*; B, *Polynoncus hemisphaericus* ; C, *Polynoncus bullatus*. Scale bar: 1 mm.

31. Thorax; posterior wings; type of merging at apex of MP venation [L = 2, CI = 50, RI = 83]

- (0) merges with other venations (Fig. 5A)
- (1) does not merge with other venations (Fig. 5B)

32. Thorax; posterior wings; location of the MP venation tip on the wing

- (0) on the lower edge of the wing (Fig. 5B)
- (1) in the middle of the wing (Fig. 5A)
- *state (0) is an autopomorphy of *Polynoncus hemisphaericus*

33. Thorax; posterior wings; fusion of RA3+4 venation before the 'pinch' [L = 1, CI = 100, RI = 100]

- (0) present (Fig. 5A)
- (1) absent

34. Thorax; posterior wings; RA3 venation [L = 2, CI = 50, RI = 83]

- (0) present (Fig. 5A)
- (1) absent

35. Thorax; posterior wings; RA4 venation [L = 1, CI = 100, RI = 100]

- (0) present (Fig. 5A)
- (1) absent

36. Thorax; posterior wings; RP venation [L = 2, CI = 50, RI = 83]

- (0) present (Fig. 5A)
- (1) absent

37. Thorax; posterior wings; RP2 venation [L = 1, CI = 100, RI = 100]

- (0) present (Fig. 5A)
- (1) absent

38. Thorax; posterior wings; MP4 venation [L = 3, CI = 33, RI = 71]

- (0) present (Fig. 5A)
- (1) absent

39. Thorax; posterior wings; fusion of RA3+4 venation [L = 2, CI = 50, RI = 83]

- (0) present (Fig. 5A)
- (1) absent

40. Thorax; posterior wings; setae at the apex of the wing

- (0) present* (Fig. 5B)
- (1) absent
- *state (0) is an autopomorphy of *Polynoncus hemisphaericus*

41. Thorax; posterior wings; setae on anterior margin [L = 1, CI = 100, RI = 100]

- (0) form a linear row of setae (Fig. 5B)
- (1) sparse and unordered setae (Fig. 5C)

42. Thorax; posterior wings; shape of wing apex

- (0) rounded (Fig. 5A–C)
- (1) pointed*
- *state (1) is an autopomorphy of *Polynoncus tenebrosus*

43. Thorax; shape of metadiscrimen area [L = 1, CI = 100, RI = 100]

- (0) rhomboidal; as wide as long (Fig. 4C)
- (1) nearly twice as wide as long (Fig. 4D)

44. Thorax; pronotum; basal tubercles [L = 3, CI = 33, RI = 0]

- (0) present (Fig. 4A)
- (1) absent

45. Thorax; pronotum; basal tubercles, shape [L = 5, CI = 20, RI = 63]

- (0) rudimentary (Fig. 4B)
- (1) well developed (Fig. 4A)

46. Thorax; pronotum; antero-lateral tubercles [L = 5, CI = 20, RI = 0]

- (0) present (Fig. 4B)
- (1) absent

47. Thorax; pronotum; shape of antero-lateral tubercles [L = 8, CI = 12, RI = 61]

- (0) prominent and well defined (Fig. 4B)
- (1) rudimentary and poorly development (Fig. 4E)

48. Thorax; pronotum; latero-basal tubercles [L = 2, CI = 50, RI = 50]

- (0) present (Fig. 4A)
- (1) absent

49. Thorax; pronotum; medial edges [L = 3, CI = 33, RI = 0]

- (0) present (Fig. 4A)
- (1) absent

50. Thorax; pronotum; surface of medial edges [L = 6, CI = 16, RI = 72]

- (0) glabrous (Fig. 4A)
- (1) covered by indument (Fig. 2E)

51. Thorax; pronotum; lateral margin [L = 1, CI = 100, RI = 100]

- (0) smooth (Fig. 4F)
- (1) bulbous (Fig. 4E)

52. Thorax; pronotum; antero-basal constriction at the lateral margin [L = 6, CI = 16, RI = 78]

- (0) present (Fig. 4E)
- (1) absent (Fig. 4F)

53. Thorax; pronotum; aspect of the antero-basal constriction at the lateral margin [L = 5, CI = 20, RI = 33]

- (0) deep (Fig. 4E)
- (1) shallow

54. Thorax; pronotum; shape of the lateral margin [L = 7, CI = 14, RI = 14]

- (0) crenulate (Fig. 4F)
- (1) smooth (Fig. 4E)

55. Thorax; pronotum; posterior margin with constriction (notched) near the posterior angles [L = 6, CI = 16, RI = 28]

- (0) present (Fig. 6A)
- (1) absent

56. Thorax; pronotum; basal tubercles and medial edge [L = 9, CI = 11, RI = 55]

- (0) connected (Fig. 6B
- (1) not connected (Fig. 6C)

57. Thorax; pronotum; antero-lateral tubercle and medial edge [L = 3, CI = 33, RI = 0]

- (0) connected (Fig. 6D)
- (1) not connected

58. Thorax; pronotum; setae on the surface of the hypomeron [L = 5, CI = 20, RI = 20]

- (0) present (Fig. 6F)
- (1) absent (Fig. 6E)
- (1) absent

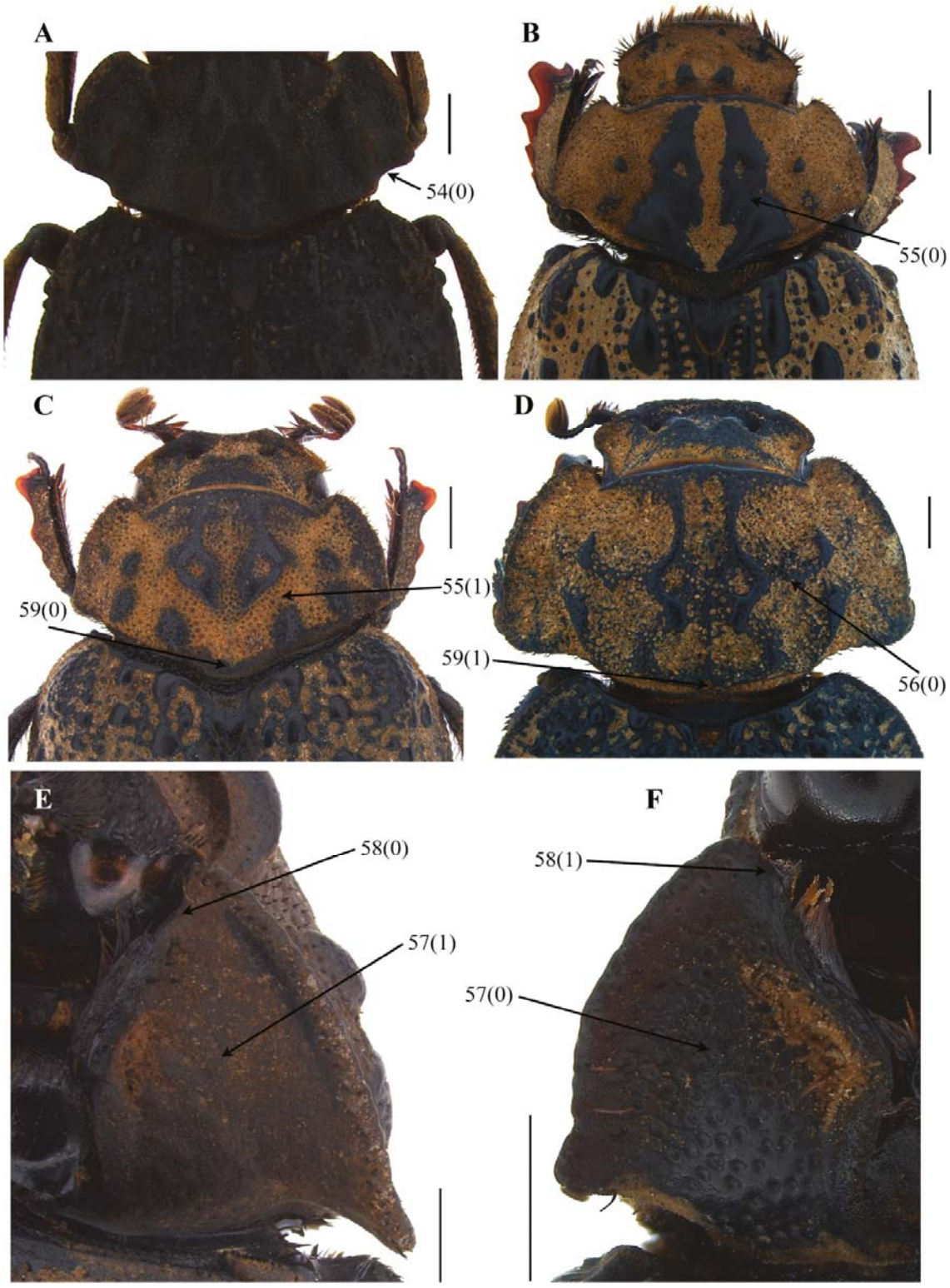

Figure 6. Characters relative of the pronotum and hypomeron of *Polynoncus*. Dorsal view of pronotum in: A, *Polynoncus chilensis*; B, *Polynoncusgemmiferus*; C, *Polynoncusargentinus*; D, *Polynoncuspatagonicus*. Hypemeron of: E, *Polynoncuspatagonicus* F, *Polynoncusgemmifer*. Scale bar: 1 mm.

59. Thorax; pronotum; emargination at the inner margin of the anterior angle of the proepisternum [L = 4, CI = 25, RI = 62]

- (0) present (Fig. 6E)
- (1) absent (Fig. 6F)

60. Thorax; pronotum; obtuse lobe projected backwards in the central portion of the posterior margin [L = 4, CI = 25, RI = 76]

- (0) present (Fig. 6C)
- (1) absent (Fig. 6D)

61. Thorax; pronotum; shape of the setae on the lateral and posterior margins [L = 1, CI = 100, RI = 100]

- (0) filiform (Fig. 4B)
- (1) spatulate (Fig. 2F)

62. Thorax; scutellum; length and width [L = 4, CI = 25, RI = 76]

- (0) longer than wide (Fig. 7A)
- (1) as long as wide (Fig. 7B)

63. Thorax; scutellum; constriction at the base of the lateral margin [L = 1, CI = 100, RI = 100]

- (0) present (Fig. 7C)
- (1) absent

64. Thorax; scutellum; anterior half of lateral margin [L = 3, CI = 33, RI = 81]

- (0) straight (Fig. 7B)
- (1) sinuous (Fig. 7A)

65. Thorax; elytra tubercles [L = 3, CI = 33, RI = 33]

- (0) present (Fig. 7D)

66. Thorax; appearance of the elytral tubercles in lateral view [L = 11, CI = 9, RI = 16]

- (0) very protruding (Fig. 7H)
- (1) little protruding (Fig. 7I)

67. Thorax; shape of elytral tubercles [L = 4, CI = 25, RI = 57]

- (0) agglutinated, coalesced (Fig. 7F)
- (1) isolated, separated (Fig. 7G)

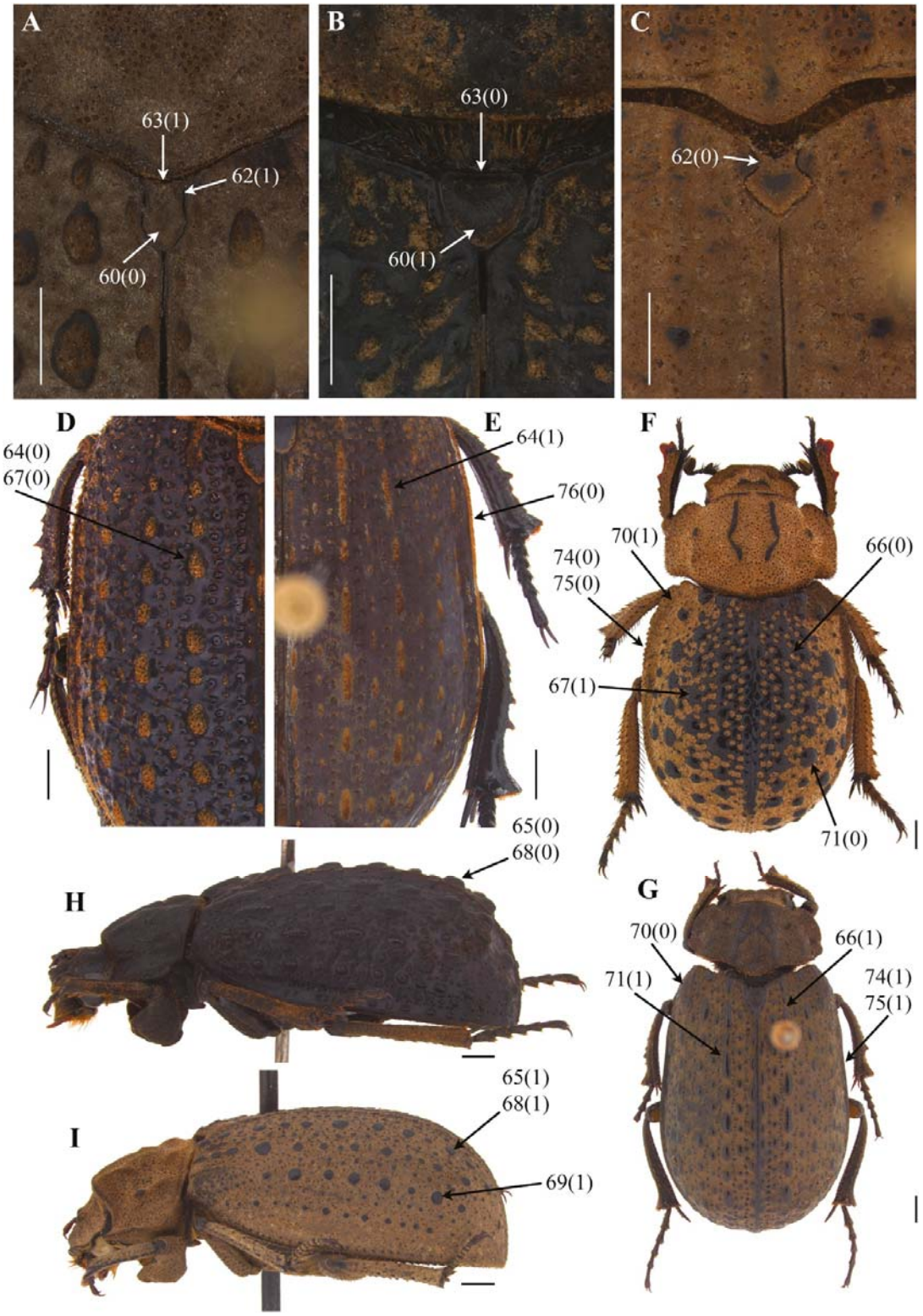

Figure 7. Characters relative of the scutellum and elytra of Trogidae. Scutellum of: A, *Polynoncus bifurcatus*; B, *Polynoncusbullatus*; C, *Omorgus suberosus*. D, left elytron of *Polynoncus pedestris*; E, right elytron of *Polynoncusdiffluens*. Dorsal habitus of: F, *Polynoncuspampeanus*; G, *Polynoncuslongitarsis*. Lateral view of: H, *Polynoncuschilensis*; I, *Polynoncusneuquen*. Scale bar: 1 mm.

68. Thorax; surface of elytra tubercles [L = 2, CI = 50, RI = 95]

- (0) velutinous (Fig. 7D)
- (1) glabrous (Fig. 7F)

69. Thorax; appearance of the surface of the elytra tubercles [L = 6, CI = 16, RI = 28]

- (0) rounded (Fig. 7H)
- (1) flattened (Fig. 7I)

70. Thorax; punctuation on the surface of elytra tubercles [L = 7, CI = 14, RI = 25]

- (0) present
- (1) absent (Fig. 7I)

71. Thorax; elytra humeral callus [L = 2, CI = 50, RI = 66]

- (0) present (Fig. 7G)
- (1) absent (Fig. 7F)

72. Thorax; shape of the odd-numbered elytra tubercles [L = 7, CI = 14, RI = 50]

- (0) rounded (Fig. 7F)
- (1) elongate (Fig. 7G)

73. Thorax; shape and size of the tubercles of the first and second elytral costae [L = 1, CI = 100, RI = 100]

- (0) similar (Fig. 8B)
- (1) differ (Fig. 8A)

74. Thorax; shape of the tubercles of the second and fourth elytral costae [L = 1, CI = 100, RI = 100]

- (0) similar (Fig. 8B)
- (1) differ (Fig. 8A)

75. Elytra; shape of lateral margin [L = 1, CI = 100, RI = 100]

- (0) margins arcuate from apex to base (Fig. 7F)
- (1) margins subparallel throughout (Fig. 7G)

76. Elytra; shape of anterior half of the lateral margin [L = 8, CI = 12, RI = 53]

- (0) crenulate (Fig. 7F)
- (1) smooth (Fig. 7G)

77. Elytral; continuous tuft of small bristles along the lateral margin [L = 5, CI = 20, RI = 75]

- (0) present (Fig. 7E)
- (1) absent

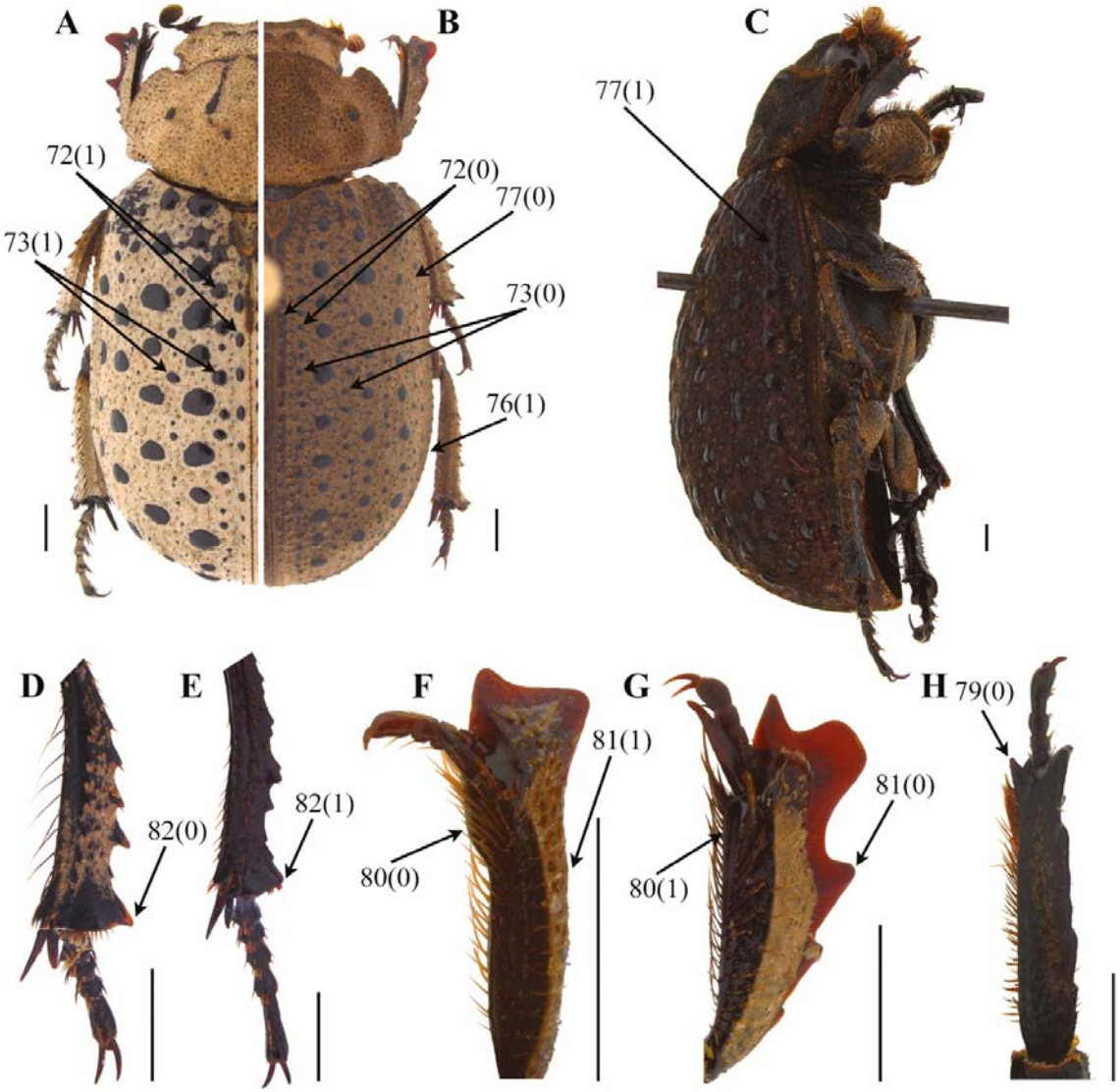

Figure 8. Characters relative of the elytra and legs of *Polynoncus*. Half left dorsal habitus of: A, *Polynoncuspseudogemmifer*; B, *Polynoncusneuquen*. C, lateral habitus of *Polynoncusaeger*. Ventral view of left mesotibia in: D, *Polynoncusperuanus*; E, *Polynoncuscrypticus*. Dorsal view of right foretibia in: F, *Polynoncusfurcillifer*; G, *Polynoncusgemmiferus*. Lateral view of right foretibia in: H, *Polynoncusgemmiferus*. Scale bar: 1 mm.

78. Elytra; subhumeral edge [L = 2, CI = 50, RI = 0]

- (0) absent
- (1) present (Fig. 8C)

79. Protibiae; longitudinal sulcus in the inner face [L = 3, CI = 33, RI = 88]

- (0) present
- (1) absent

80. Protibiae; teeth in the apex of dorsal surface [L = 5, CI = 20, RI = 71]

- (0) present (Fig. 8H)
- (1) absent

81. Protibiae; callus in the apex of inner margin [L = 1, CI = 100, RI = 100]

- (0) present (Fig. 8F)
- (1) absent (Fig. 8G)

82. Protibias; second teeth in the inner margin [L = 2, CI = 50, RI = 0]

- (0) present (Fig. 8G)
- (1) absent (Fig. 8F)

83. Mesotibias; tooth in the apex of outer margin in ventral view [L = 4, CI = 25, RI = 72]

- (0) absent (Fig. 8E)
- (1) present (Fig. 8D)

84. Aedeagus; medial lobe with a dorsal portion surrounding the soft parts [L = 1, CI = 100, RI = 100]

- (0) present (Fig. 9B)
- (1) absent (Fig. 9A)

85. Aedeagus; dorsal portion of median lobe forked in the middle [L = 1, CI = 100, RI = 100]

- (0) present (Fig. 9C)
- (1) absent (Fig. 9B)

86. Aedeagus; dorsal portion of median lobe; shape of lateral margins at the middle [L = 2, CI = 50, RI = 80]

- (0) symmetrical (Fig. 9E)
- (1) asymmetrical (Fig. 9D)

87. Aedeagus; dorsal portion of median lobe; wide apex in dorsal view [L = 6, CI = 16, RI = 68]

- (0) absent (Fig. 9G)
- (1) present (Fig. 9E)

88. Aedeagus; dorsal portion of median lobe; general shape [L = 1, CI = 100, RI = 100]

- (0) simple, without ornaments, and symmetric (Fig. 9F)
- (1) complex, with distinct forms and ornaments, usually asymmetric (Fig. 9J)

89. Aedeagus; dorsal portion of median lobe; dorsal surface with blade-like shape [L = 1, CI = 100, RI = 100]

- (0) absent
- (1) present (Fig. 9G, H)

90. Aedeagus; dorsal portion of median lobe; apex with a spoon-like shape in lateral view [L = 4, CI = 25, RI = 62]

- (0) absent
- (1) present (Fig. 9I)

91. Aedeagus; phallobase; length [L = 12, CI = 16, RI = 54]

- (0) half of total aedeagus length (Fig. 9J)
- (1) one-third of total aedeagus length (Fig. 9E)
- (2) quarter of total aedeagus length (Fig. 9I)

92. Aedeagus; phallobase distinctly arched in lateral view [L = 1, CI = 100, RI = 100]

- [1] present (Fig. 9K)
- [2] absent (Fig. 9I)

93. Aedeagus; phallobase at the middle in dorsal view [L = 2, CI = 50, RI = 83]

- (0) completely fused (Fig. 9L)
- (1) with a membranous portion (Fig. 9F)

94. Aedeagus; parameres; apex torsion inward [L = 5, CI = 20, RI = 63]

- (0) present (Fig. 9C)
- (1) absent (Fig. 9J)

95. Aedeagus; parameres fully sclerotized [L = 6, CI = 16, RI = 66]

- (0) absent
- (1) present (Fig. 9K)

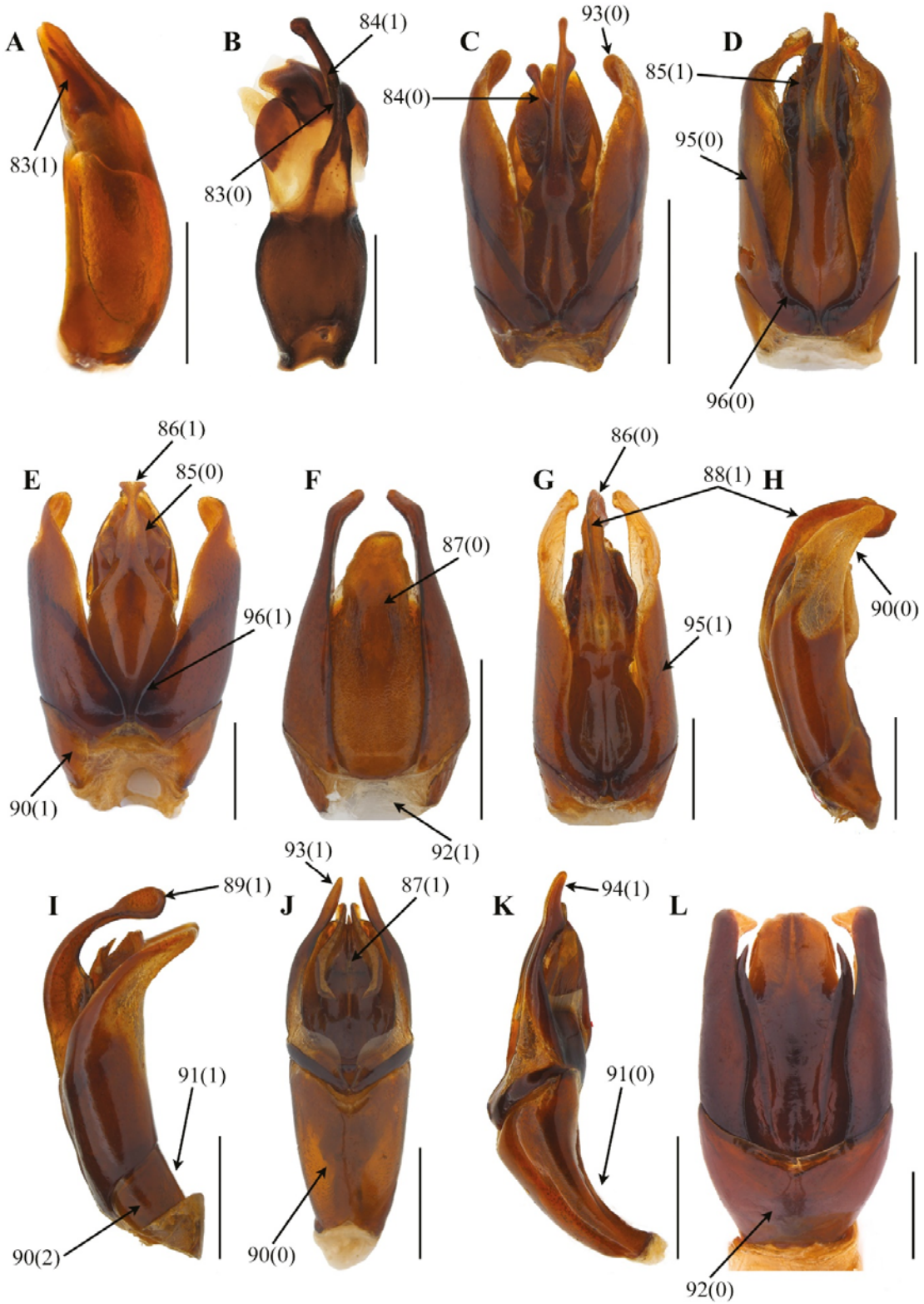

Figure 9. Characters relative of male genitalia of Trogidae. Median lobe (with parameres removed, of: A, *Omorgus suberosus*; B, *Polynoncus vazdemelloi*. Aedeagus habitus of: C, *Polynoncusfurcillifer*; D, *Polynoncuspilularius*; E, *Polynoncuspatriciae*; F, *Omorgus batesi*. Dorsal (G) and (H) lateral views of *Polynoncus ecuadorensis*. I, lateral view of *Polynoncusneuquen*. Dorsal (J) and (K) lateral views of *Phoberus luridus*. Dorsal view of L, *Omorgus squalidus*. Scale bar: 1 mm.

96. Aedeagus; sclerotized transversal band in the middle of parameres [L = 3, CI = 33, RI = 85]

- (0) present (Fig. 9D)
- (1) absent (Fig. 9G)

97. Aedeagus; inner margin of parameres; near of the base [L = 5, CI = 20, RI = 66]

- (0) curve, ~90º (Fig. 9D)
- (1) ~180º (Fig. 9E)

98. Larvae; spiracle type (Scholtz 1986) [L = 1, CI = 100, RI = 100]

- (0) biforous
- (1) cribriform

Phylogenetic results

Different topologies were obtained from the MP analysis conducted under EW and IW. The EW analysis yielded 24 most-parsimonious trees with 306 steps (CI = 33; RI = 70). The consensus tree of EW showed a lack of resolution among genera within the Omorginae clade, but better resolved the distal clades. Of the 11 *k*-values obtained from the IW analysis search, five yielded an equal highest SPR score, with 100% similarity (Supporting Information, Table S3). Therefore, the mean of the five highest scoring *k*-values ($k = 2.762$) was used. The final hypothetical model of phylogenetic reconstruction was thus obtained using a *k*-value of 2.762 and 310 steps (Fit = 29.976; CI = 32; RI = 69). As the topology generated by the IW method was better solved and supported than that of the EW method, the IW model was here used for inference on the phylogenetic relationships among *Polynoncus* species.

Discussion

Outgroup

The monophyly of Trogidae retrieved here corroborates previous phylogenetic studies (e.g. Scholtz 1986, d'Hotman and Scholtz 1990, Scholtz and Peck 1990, Browne *et al*. 1993, Strümpher *et al*. 2014) and is aligned with the current classification of the subfamilies proposed by Nikolajev (2005). Troginae, composed by the genera *Trox* and *Phoberus*, and Omorginae, composed by the genera *Omorgus* and *Polynoncus*, were retrieved as a sister-group in both EW and IW analyses (Fig. 10).

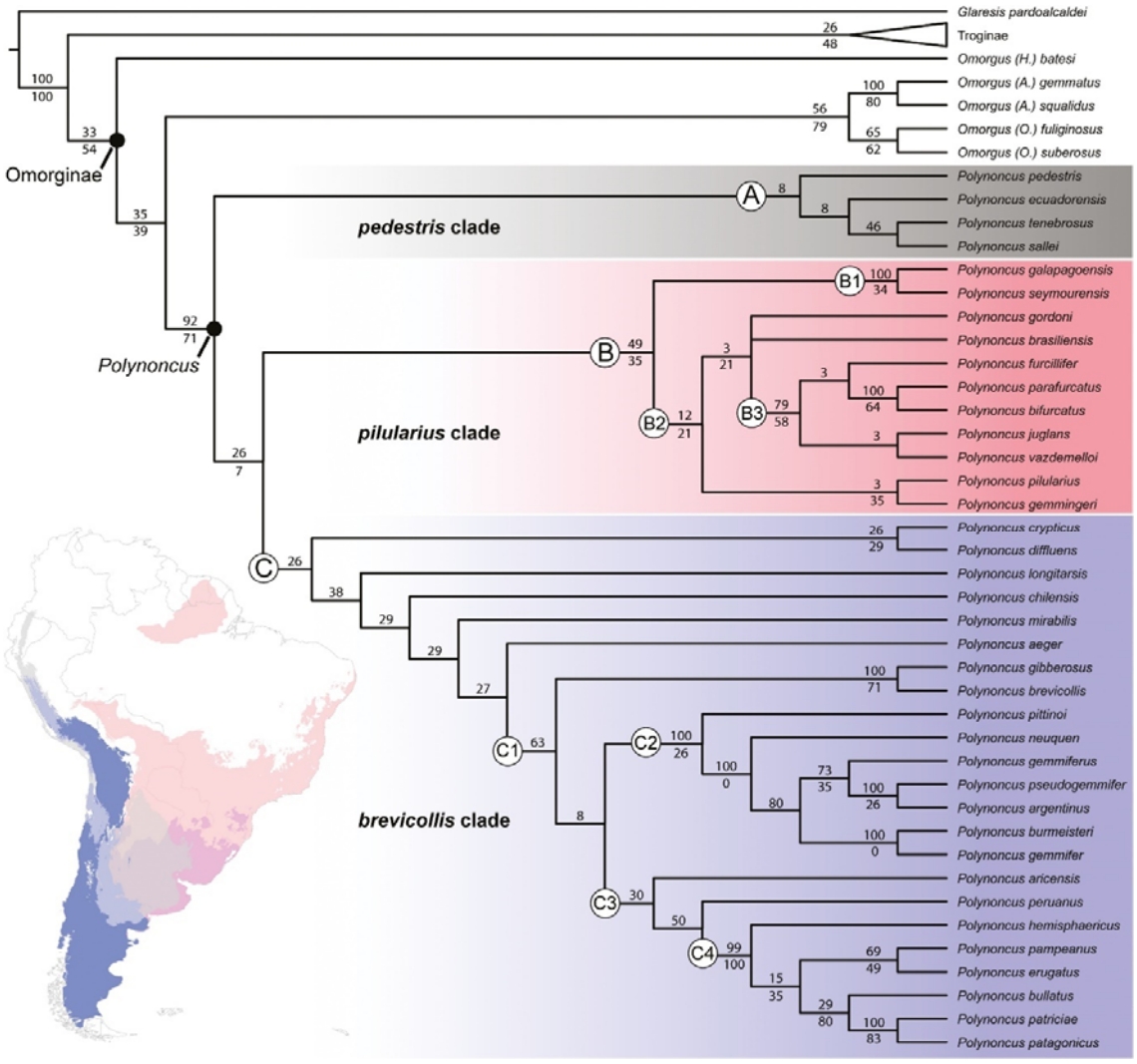

Figure 10. Hypothetical reconstruction of the relationships of *Polynoncus* based on the strict consensus tree under implied weight (k = 2762). Values of clade supported obtained by RBS and SR analyses are given above and below the branches, respectively. The scheme shows three lineages (*pedestris*, *pilularius*, and *brevicollis* clades) retrieved in the analysis and the geographical distribution in the South America region.

The phylogenetic relationships between *Omorgus* and *Polynoncus* is well defined with morphological (Scholtz 1986, Scholtz and Peck 1990) and molecular (Strümpher *et al*. 2014) evidence. Considering the occurrence of the genera *Omorgus* and the endemic *Polynoncus* in South America (Vaurie 1962, Scholtz 1990, Costa-Silva *et al*. 2024), Scholtz (1986) hypothesized that both genera evolved from an *Omorgus*-like ancestor. This hypothesis was later tested with molecular evidence by Strümpher *et al*. (2014), indicating that *Omorgus* and *Polynoncus* diverged from their common ancestor *c*. 117 Mya (for details, see: Strümpher *et al*. 2014, 2016).

The results of our analysis indicate that *Omorgus* is a non-monophyletic group, contradicting the Scholtz (1986) hypothesis. However, a proposal for a new classification of *Omorgus* is beyond the scope of this study. An additional molecular phylogeny of the family Trogidae is

currently underway by the first two authors (V.C.S. and W.P.S.) to propose a new classification change within Omorginae.

Phylogenetic relationships within *Polynoncus*

Under both phylogenetic analyses (EW and IW), *Polynoncus* was recovered as monophyletic, corroborating the hypotheses of previous research on the genus (*e.g.*Scholtz 1986, Scholtz and Peck 1990, Browne *et al*. 1993, Strümpher *et al*. 2014). Nonetheless, only the topology obtained from the IW model will be discussed here, as the resolution and level of support were better solved than that of the EW model (Fig. 10). *Polynoncus* monophyly was well supported (RBS = 92; SR = 71), with five synapomorphies (the last one homoplastic): presence of the one single seta in the sixth antennomere (3:0—Fig. 1A); clypeus with apical portion downward abruptly (20:0—Fig. 2A); aedeagus with a medial lobe and a dorsal portion surrounding the soft parts (83:0—Fig. 9B); parameres not fully sclerotized (92:1—Fig. 9F); and with apical torsion inward (93:0—Fig. 9C).

The presence of one single seta in the sixth antennomere was first documented by Costa-Silva *et al*. (2024) and used as differential diagnosis for the *Polynoncus* species. The apical portion of the clypeus slopes downward abruptly (forming a straight angle with the front—Fig. 2A) is historically used to separate *Polynoncus* from *Omorgus* in identification keys (e.g. Vaurie 1962, Scholtz 1986, 1990, Gómez 2008, Almeida and Mise 2009, Strümpher *et al.* 2016, Costa-Silva *et al.* 2024a). d'Hotman and Scholtz (1990) mentioned that parameres with inward apical torsion is a synapomorphy of Omorginae. However, in this study, this characteristic was observed just in *Polynoncus* species, indicating that parameres with apical torsion inward is a derived condition (apomorphic), while the primitive one (apex with straight shape) is found in *Omorgus* and other genera of Trogidae.

Within the *Polynoncus* clade, three lineages were retrieved and will be hereafter treated as *pedestris* (A), *pilularius* (B), *brevicollis* clades (C), and their respective subclades (e.g. B1, B2, C1, etc.). The *pedestris* clade presented a low branch support (RBS = 8) with three synapomorphies (all homoplastic) (Fig. 11): antero-basal constriction with shallow shape (52:1), basal tubercles and medial edge of pronotum not connected (55:1—Fig. 6C), and the presence of a longitudinal sulcus in the inner face of protibial (78:0). Into this clade, *Polynoncus pedestris* is retrieved as a sister-group of *P. ecuadorensis* + (*P. tenebrosus* + *P. sallei*). This last subclade (*ecuadorensis* + (*tenebrosus* + *sallei*)) is supported by three synapomorphies (the last two being homoplastic) with low branch support (RBS = 8): dorsal surface of a median lobe with a blade-like shape (88:1—Fig. 9G, H); apex of the median lobe with a spoon-like shape in lateral view (89:1—Fig. 9I); and the inner margin of parameres curve near of the base (96:0—Fig. 9D). Even with markable external diagnostic characteristic to separate these three species (see diffential diagnostic in: Costa-Silva *et al.* 2024a), the spoon-like shape of the median lobe of those three species as a synapomorphy, and the shared geographical distribution from the highest regions of the north-west of the Andean Mountains (Peru and Ecuador) suggest an evolutive relationship between these species.

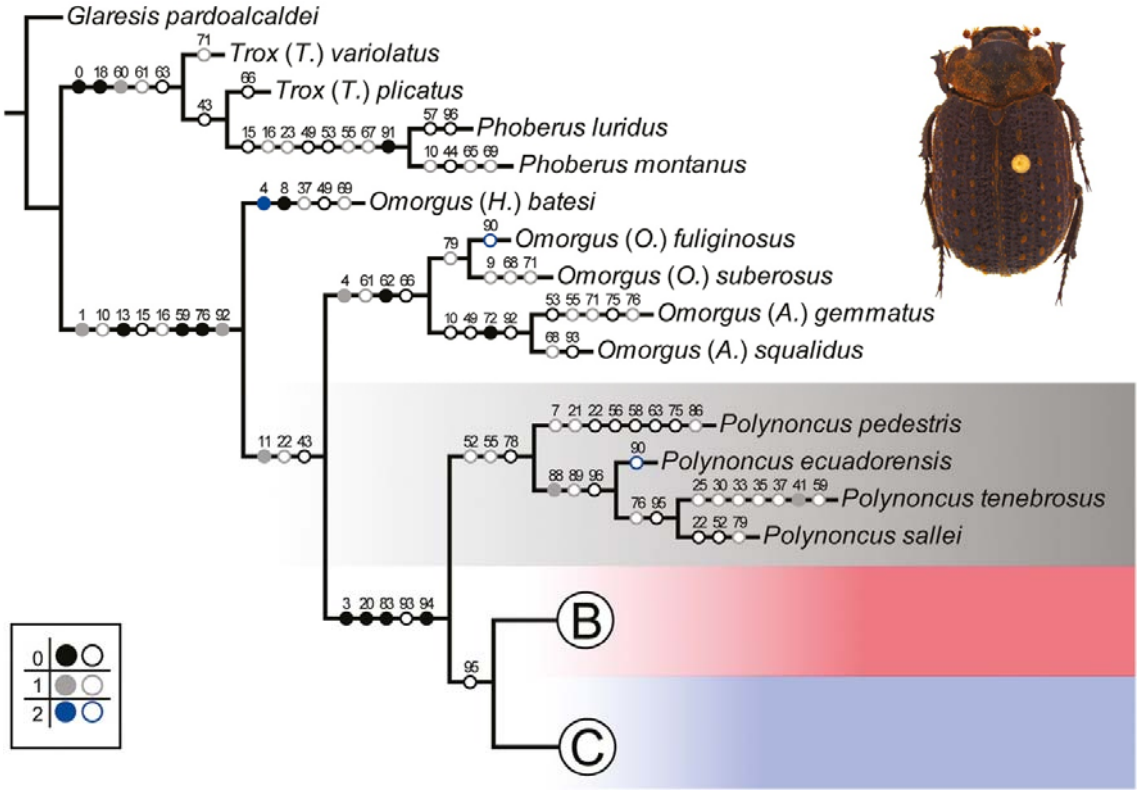

Figure 11. Part of the strict consensus tree from two most parsimonious trees showing the phylogenetic relationships of species of the outgroup and '*pedestris* clade'. (Full circles indicate synapomorphies, while empty white circles indicate homoplastic synapomorphies. Black colour refers to state '0'; grey refers to state '1'; and blue refers to state '2'. Image: *Polynoncus pedestris*.

The *pilularius* clade (B) is better supported than the *pedestris* clade (A) and includes all species with asymmetrical male genitalia (RBS = 49; SR = 35) (Fig. 10). Four synapomorphies, two of which were homoplastic (characters 79 and 90), supported this clade (Fig. 12): a right mandible with a raised swelling parallel with outer margin (17:0—Fig. 3E), protibiae without an apical tooth in the dorsal surface (79:1), dorsal portion of median lobe with asymmetrical lateral margins at the middle (85:1—Fig. 9D), and phallobase with a quarter of total aedeagus length (90:2—Fig. 9I).

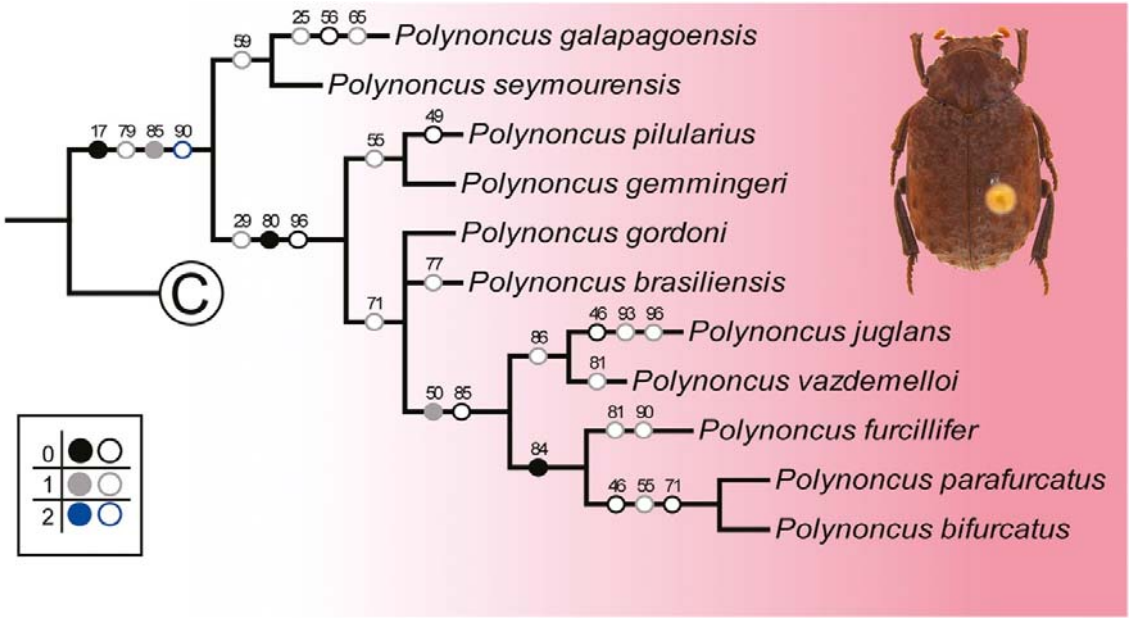

Figure 12. Part of the strict consensus tree from two most parsimonious trees showing the phylogenetic relationships of species of the outgroup and '*pilularius* clade'. (Full circles indicate synapomorphies, while empty white circles indicate homoplastic synapomorphies. Black colour refers to state '0'; grey refers to state '1'; and blue refers to state '2'. Image: *Polynoncus vazdemelloi*.

Two subclades (B1 + B2—Fig. 10) can be recognized within '*pilularius*' (B) clade. The subclade B1 include the species *Polynoncus galapagoensis* and *P. seymourensis*, the only *Polynoncus* species to occur in the Galapagos Islands (Vaurie 1962, Scholtz 1990b, Costa-Silva *et al.* 2024a). Considering the restricted geographical distribution of both species (both being confined to the Galapagos Islands), Vaurie (1962) and Scholtz (1986, 1990b) hypothesized that both species share a common ancestor. The highest branch support of our results (RBS = 100; SR = 34) corroborates this hypothesis (Fig. 10). Furthermore, *Polynoncus galapagoensis* presents reduced membranous wings, suggesting that the fully winged *P. seymourensis* is more primitive and responsible for the dispersion of these species among islands (Costa-Silva *et al.* 2024a), while the wingless *P. galapagoensis* is more derived and has lost its flight capacity due to environmental pressures [i.e. restricted areas (islands, mountains), wind, temperature, etc.; for more details, see: Darlington (1943), Scholtz (1981)]. Probably as a result of loss of flight capacity, *P. galapagoensis* is found restricted to the small and isolated northern islands of Galapagos (Costa-Silva *et al.* 2024a).

The subclade B2 (RBR = 12; SR = 21) (Fig. 12) is supported in the presence of the apical callus in the inner margin of protibiae (80:0—Fig. 8F). This characteristic is mentioned here for the first time in the literature and can be used to distinguish this group from the remaining species of *Polynoncus*. Also, two homoplasies with phylogenetic signal were identified here: the length of AA1+2 venation is a quarter of AA3+4 length (29:1—Fig. 5A) and the inner margin of the parameres, near to the base, form a curve of ~90° (96:0—Fig. 9D). All species that composed the subclade B2 are insular, and most of them occur within tropical regions (Brazil, Paraguay, Bolivia, Uruguay, and north-east Argentina). *Polynoncus gemmingeri* + *P. pilularius* clade (RBS = 3; SR = 35) is recognized as a sister-clade of all remaining species, distinguished by an asymmetrical superior lobe of the aedeagus (Fig. 10). The subclade B3 (RBS = 79; SR = 58) is a monophyletic and well-supported group with the lateral margin of

pronotum bulbous located in front of the central portion (50:1—Fig. 4E), and symmetrical lateral margins at the middle of the superior lobe of aedeagus (85:0—Fig. 9E). These characteristics may also be used to distinguish the species' group morphologically (Vaurie 1962) and are included in a dichotomous key for species' identification or differential diagnosis (i.e. Pittino 1987, Scholtz 1990b, Gómez 2008, Costa-Silva and Diéguez 2020, Costa-Silva *et al*. 2024a). Even without a formal hypothesis of homology, the arrangements of the terminals present in the identification keys presented by Scholtz (1990b) and, more recently, by Costa-Silva *et al.* (2024a) are similar to the topologies presented here.

The *brevicollis* clade (C) (Fig. 13) is composed of species distributed across Chile, Argentina, and Uruguay (Fig. 10). This clade is supported with two synapomorphies (all homoplastic) (RBS = 26): pronotum with a surface of medial edges glabrous (49:0—Fig. 4A) and odd-numbered tubercles of elytra with elongate shape (71:1—Fig. 7G). With few exceptions, the species that compose clade C are the same as those cited by Haaf (1953) and Vaurie (1962) as '*brevicollis*-group' in their studies of the global and South American Trogidae species, respectively. Even so, the diagnostic characteristics used by those authors to recognize the *brevicollis*-group [i.e. presence of humeral callus (70:0—Fig. 7G); margins of elytra subparallel (74:1—Fig. 7G) and metasternum as wide as long (rhomboidal) (42:0—Fig. 4D)] were not retrieved as a synapomorphy of this group in this study.

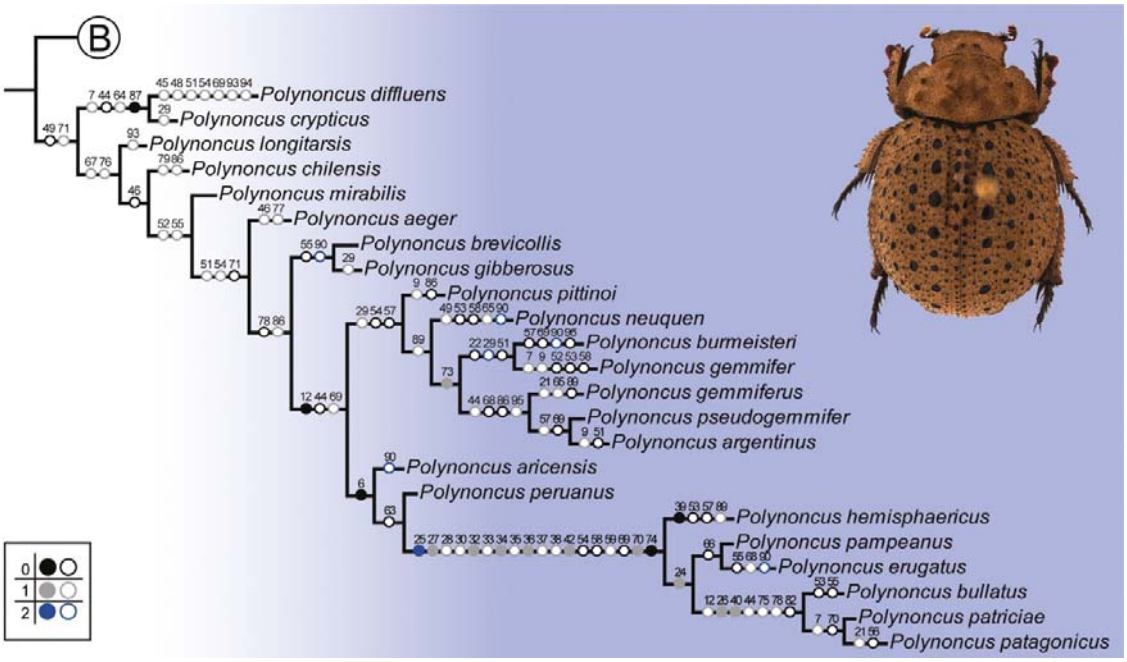

Figure 13. Part of the strict consensus tree from two most parsimonious trees showing the phylogenetic relationships of species of the outgroup and '*brevicollis* clade'. (Full circles indicate synapomorphies, while empty white circles indicate homoplastic synapomorphies. Black colour refers to state '0'; grey refers to state '1'; and blue refers to state '2'. Image: *Polynoncus hemisphaericus*.

Within clade C, the species *Polynoncus diffluens* + *P. crypticus* are retrieved as a sister-clade of the other species of the group (Fig. 13). The dichotomy of *P. diffluens* + *P. crypticus* is supported with four synapomorphies, the first three being homoplastic: shape of anterior margin of labrum symmetric (7:1– Fig. 1D); basal tubercles of pronotum rudimentary (44:0—

Fig. 4B); absence of elytral tubercles (64:1); and dorsal portion of median lobe simple, without ornaments and symmetric (87:0—Fig. 9F). According to Diéguez (2019), *P. diffluens* and *P. crypticus* present a similar morphology that can be easily confused at first glance. Moreover, both species share a morphological characteristic not typical for *Polynoncus* species: male genitalia are compact and simple, and there is an absence of elytral tubercles. As mentioned by Vaurie (1962), the male genitalia of *Polynoncus* species are rather complex, with a dorsal (usually asymmetrical and variable) portion surrounding the soft parts (also see: Pittino 1987). This complexity of the aedeagus shape was treated as a synapomorphy of *Polynoncus* by Scholtz (1986). However, the male genitalia of *P. diffluens* and *P. crypticus* lack the ornaments and bizarre structures on the dorsal portions, instead assuming a compact and simple shape typical of those found in *Omorgus* species; a plesiomorphic condition suggested by Scholtz (1986). The hypothesis of homology of this character showed a great phylogenetic signal that both species evolved from a common ancestor, and the lack of ornaments in the dorsal portion of aedeagus was result of a secondary lost by phylogenetic reversion (or atavism).

The subclade C1 (RBS = 63) is supported with two synapomorphies (all homoplastic): presence of a longitudinal sulcus in the inner face of the protibiae (78:0); and apical part of median lobe wide in dorsal view (86:1—Fig. 9E). Two lineages of C1 are recognized (Figs 10, 13): subclade *P. brevicollis* + *P. gibberosus* + (C2 + C3). All species of these subclades are restricted to Argentina and/or Chile (Diéguez 2008; also see: Costa-Silva *et al.* 2024a). Both *P. brevicollis* and *P. gibberosus* are morphological related species as discussed by Scholtz (1990) and Costa-Silva *et al.* (2024a). The lineage C2 + C3 (RBS = 8) is supported with three synapomorphies, the last two of which are homoplastic: fourth maxillary palpomere with a sinuosity in the ventral margin near the apex (12:0—Fig. 3A); basal tubercles of pronotum rudimentary (44:0—Fig. 4B); and absence of punctuation in the surface of tubercles (69:1—Fig. 7I).

The subclade C2 (RBS = 100; SR = 26) is a well-supported clade of Argentinean species (with the exception of *P. burmeisteri*, which also occurs in Bolivia—see: Costa-Silva *et al.* 2024a) with three synapomorphies (all homoplastic): AA1+2 venation of wings with a quarter of AA3+4 length (29:1—Fig. 5A); posterior margin of pronotum with constriction (notched) near the angles (54:0—Fig. 6A); and surface of hypomeron with setae (57:0—Fig. 6F). This group of species (C2) is also supported by the taxonomic history proposed by several authors, where the similarity of morphological characteristic put all species together in the identification key and/or differential diagnosis (i.e. Vaurie 1962, Scholtz 1990b, Costa-Silva and Diéguez 2020, Costa-Silva *et al*. 2024a). In both dichotomous keys for *Polynoncus* species, one carried out by Vaurie (1962) and the other by Costa-Silva *et al.* (2024a), the authors used the presence of a tooth in the apex of the outer margin of the mesotibia to separate this group from other congeneric species. However, even though it is a good taxonomical characteristic for identification purposes, this character was retrieved as homoplastic (also present in *P. peruanus*).

The subclade C3 (RBS = 30) is supported with only one synapomorphy (Fig. 13): the interocular distance four or five times the length of the eyes (Fig. 2C). According to Vaurie (1962), this characteristic corresponds to the '*bullatus* group', where the species are distinguished by the absence of a humeral callus and reduced or absent wings (as those from the subclade C4). However, the related species *P. peruanus* and *P. aricensis*, both macropterous, also present small eyes, contradicting the diagnostic characteristic of Vaurie (1962) and Haaf (1953) for the '*bullatus* group'. The true '*bullatus*' group (*sensu* Vaurie 1962) is retrieved here as monophyletic under the subclade C4 (RBS = 99; SR = 100). This well-

defined subclade is supported with 18 synapomorphies, being the characters 28, 30, 33, 35, 37, 38, 54, 58, 59, and 69, homoplastic (Fig. 13): vestigial posterior wings (25:2—Fig. 5C); the constriction between RA3+4, RA3, and RA4 venation ('pinch') absent (27:1); absence of AA1+2 venation (28:1); end of MP venation not fusing with any venations (30:1—Fig. 5B); absence of fusion of the RA3+4 venation before the 'pinch' (32:1); absence of the RA3 venation (33:1); absence of the RA4 venation (34:1); absence of the RP venation (35:1); absence of the RP2 venation (36:1); absence of the MP4 venation (37:1); absence of the fusion of RA3+4 venation (38:1); shape of metadiscrimen area nearly twice as wide as long (42:0—Fig. 4C); posterior margin with a constriction (notched) near the angles (54:0—Fig. 6A); presence of an emargination in the internal margin of anterior angle of proepisternum (58:0—Fig. 6E); absence of a posterior margin projecting backward in obtuse lobe at the middle (59:1—Fig. 6C); presence of the punctuation in the surface of tubercles (69:0); absence of a humeral callus (70:1—Fig. 7F); and elytral with margins arcuate from apex to base (74:0—Fig. 7F).

The last two characters (70 and 74) were also cited by Vaurie (1962), Scholtz (1990), Gómez (2008), and Costa-Silva *et al.* (2024a) in their respective identification keys for *Polynoncus* species. However, these characters are not a true synapomorphy of *Polynoncus* when compared with other wingless species of Trogidae (Scholtz 1981, 2000, Browne *et al*. 1993). Groups of wingless species of the family are reported from different zoogeographical regions [e.g. *Omorgus* (*O*.) *pastillarius* (Blanchard, 1847) from South America; *Omorgus* (*O*.) *dohrni* (Harold, 1872) from Australia; *Phoberus natalensis* (Haaf, 1954) from the Afrotropical region], suggesting that loss of flight appeared many times during the evolution of the group. According to Scholtz (1981), the reduction of the wings can often be correlated with the locality and habit of the species (i.e. mountains, deserts, or islands; for additional details, see: Roff 1990). As these environments are stable and favourable for the group (e.g. there are readily available food sources), the species do not need to disperse to search for new habitats (Aukema 1990). Due to this selective pressure or occupation, some morphological structures of beetles' wings were lost, termed atrophy (Fiori 1977, Wagner and Liebherr 1992, Browne *et al*. 1993).

As also discussed by Scholtz (1981), wingless species of Trogidae are often reported within desert and arid regions (i.e. North America, Africa, and Australia). These reports match with the geographical distribution of the wingless *Polynoncus* in South America, mainly in arid regions of Argentina and Chile (Costa-Silva *et al.* 2024a). Therefore, as occurs in other Coleoptera species, the wingless species of *Polynoncus* are often large (up to 1.5 mm), relative to the macropterous species (0.6–1.5 mm) (Scholtz 1981). In addition, these species also present a short metasternum, reduced scutellum, absence of humeral callus, and small eyes, in accordance with all non-related species that live in similar regions of the world. For a comprehensive study about the flightless species of Trogidae, see Scholtz (1981) and Browne *et al*. (1993).

Conclusion

In this study, we have provided the first hypothetical reconstruction of the genus *Polynoncus* based solely on morphological data, presenting the first evidence for the evolutionary relationships between the species of *Polynoncus*. The genus *Polynoncus* was retrieved as monophyletic and as a sister-group of the paraphyletic genus *Omorgus* ((*Omorgus* + *Afromorgus*) + subgenus *Haroldomorgus*)). The synapomorphies that support the monophyly of *Polynoncus* cited by previous authors (Scholtz 1986, Browne *et al*. 1993, Strümpher *et al*. 2014) were here tested and established based on a large set of species, thus

corroborating the evolutionary hypothesis for the group (for a hypothesis of origin and dispersal of *Polynoncus*; see: Strümpher *et al*. 2014).

Whitin the *Polynoncus* clade, three major lineages are recognized: '*pedestris*', '*brevicollis*', and '*pilularius*' clade (Fig. 10). Each clade is composed of species with a similar geographical distribution in South America, suggesting a pattern of dispersal from the temperate to the tropical zones as previous cited by Costa-Silva *et al.* (2024a). Further studies with a molecular and/or biogeographic approach could give us an alternative hypothesis about origin, dispersal, and relationship between species of *Polynoncus* and related taxa in South America, and may help to further resolve the phylogeny of the genus.

Acknowledgements

We are grateful to Thadeu Sobral-Souza (UFMT), Rafael Sousa (MZSP), Mario Cupello (TAMU), Vinicius Ferreira (SDEI), and Angélico Asenjo (ITV) for all their support during this study, and all the collection curators mentioned in the Materials and methods section. Thanks to Ciar Noble for providing the revision of English. Special thanks to Gimo Daniel (National Museum, Bloemfontein), Paschoal Grossi (UFRPE), André Freitas (UNICAMP), and Jessie Pereira (UNICAMP) for comments and suggestions on the first draft of this manuscript. This study was financed by the Coordenação de Aperfeiçoamento de Pessoal de Nível Superior—Brasil (CAPES)—Finance Code 001 (process nº: 88882.435386/2019-01). V.C.S. thank to Ernst Mayr Grants (Harvard University) and the Stewart and Jarmila Peck Visiting Scientist Awards in Entomology (Canadian Museum of Nature) for the financial support to visit the Muséum National d'Histoire Naturelle (Paris, France), the Natural History Museum (London, England), and the Canadian Museum of Nature (Ottawa, Canada). F.Z.V.M. thanks the National Council for Scientific and Technological Development (CNPq), process number 431760/2018-7, 306745/2016-0, 248299/2012-3. Project SISGEN nº A97BAB4. The authors thank Dr Andrey Frolov (Russian Academy of Sciences) and Prof Catherine Sole (University of Pretoria) for their important comments and suggestions that improved the manuscript.

CRediT statement

Vinícius da Costa-Silva (conceptualization, data curation, formal analysis, investigation, methodology, validation, writing-original draft, writing-review and editing), Werner P. Strümpher (conceptualization, investigation, validation, writing—review and editing), Patricia J. Thyssen (conceptualization, project administration, validation, writing—review and editing), and Fernando Z. Vaz-de-Mello (conceptualization, methodology, project administration, validation, writing—review and editing). All authors have read and agreed to the published version of the manuscript.

Conflict of interest

The authors state that they have no conflict of interest.

DATA AVAILABILITY

The data underlying this article are available in the article and in its online supplementary material.

References

Almeida LM, Mise KM. Diagnosis and key of the main families and species of South American Coleoptera of forensic importance. Revista Brasileira de Entomologia 2009; 53:227–44. https://doi.org/10.1590/S0085-56262009000200006

Aukema B. Wing-length determination in two wing-dimorphic *Calathus* species (Coleoptera: Carabidae). *Hereditas* 1990; 113:189–202. https://doi.org/10.1111/j.1601-5223.1990.tb00084.x

Ballerio A, Krell FT, Randrianirina JE et al. Rediscovery of the enigmatic Madagascan endemic *Belohina inexpectata* Paulian, 1958, with notes on its morphology and phylogenetic position (Coleoptera, Scarabaeoidea: Belohinidae). *Fragmenta Entomologica* 2023; 55:139–60.

Beutel RG, Yavorskaya M. Structure and evolution of mouthparts in Coleoptera. In: Krenn HW (ed.), *Insect Mouthparts: Form, Function, Development and Performance*. Zoological Monographs, Vol. 5. Switzerland: Springer Nature, 2019, 387–418.

Blanchard CÉ. Insectes de l'Amérique Méridionale. In: d'Orbigny A, Blanchard CÉ, Brullé A (eds), *Voyage dans l'Amérique Méridionale*. Vol. 6, Part 2, livraison 90. Paris, France: P. Bertrand, 1847, 185–232.

Browne DJ, Scholtz CH. The morphology and terminology of the hindwing articulation and wing base of the Coleoptera, with specific reference to the Scarabaeoidea. *Systematic Entomology* 1994; 19:133–43. https://doi.org/10.1111/j.1365-3113.1994.tb00583.x

Browne DJ, Scholtz CH. Phylogeny of the families of the Scarabaeoidea (Coleoptera) based on characters of the hindwing articulation, hindwing base and wing venation. *Systematic Entomology* 1995; 20:145–73. https://doi.org/10.1111/j.1365-3113.1995.tb00089.x

Browne DJ, Scholtz CH. A phylogeny of the families of Scarabaeoidea (Coleoptera). *Systematic Entomology* 1999; 24:51–84.

Browne DJ, Scholtz CH, Kukalova-Peck J. Phylogenetic significance of wing characters in the Trogidae (Coleoptera: Scarabaeoidea). *African Entomology* 1993; 1:195–206.

Burmeister HCC. Die Argentinischen Arten der Gattung Trox Fabr. *Entomologische Zeitung* 1876; 37:241–68.

Caveney S, Scholtz CH. Evolution of ommatidium structure in the Trogidae (Coleoptera). *Systematic Entomology* 1993; 18:1–10. https://doi.org/10.1111/j.1365-3113.1993.tb00652.x

Costa-Silva V, Diéguez VM. A new species of *Polynoncus* Burmeister (Coleoptera: Trogidae) from Argentina. *Zootaxa* 2020; 4868:267–74.

Costa-Silva V, Strümpher WP, Thyssen PJ et al. Taxonomic revision of the South American genus Polynoncus Burmeister, 1876 (Coleoptera: Scarabaeoidea: Trogidae). *Journal of Natural History* 2024a 58:14–166. https://doi.org/10.1080/00222933.2023.2260060

Costa-Silva V, Strümpher WP, Barclay MVL et al. An illustrated catalogue of South American species of Omorgus Erichson, 1847 (Coleoptera, Trogidae, Omorginae) including a neotype designation and taxonomical changes. *Contributions to Entomology* 2024b; 74:81–101. https://doi.org/10.3897/contrib.entomol.74.e126799

Cristóvão JP, Vaz-de-Mello FZ. The terminalia of the superfamily Scarabaeoidea (Coleoptera): specific glossary, dissecting methodology, techniques and previously unrecorded sexual dimorphism in some difficult groups. *Zoological Journal of the Linnean Society* 2020; 191:1001–43. https://doi.org/10.1093/zoolinnean/zlaa079

Darlington PJ. Carabidae on mountains and islands: data on the evolution of isolated faunas, and on atrophy of wings. *Ecological Monographs* 1943; 13:37–61. https://doi.org/10.2307/1943589

Diéguez VM. Conocimiento actual de los Trogidae de Chile (Coleoptera: Scarabaeoidea). *Revista Chilena de Entomología* 2008; 34:11–28.

Diéguez VM. Nueva especie del género Polynoncus Burmeister (Coleoptera: Trogidae) para Chile. *Revista Chilena de Entomología* 2019; 45:87–92.

Dietz L, Seidel M, Eberle J et al. A transcriptome-based phylogeny of Scarabaeoidea confirms the sister group relationship of dung beetles and phytophagous pleurostict scarabs (Coleoptera). *Systematic Entomology* 2023; 48:672–86. https://doi.org/10.1111/syen.12602

Erichson WF. Conspectus coleopterorum quae in Republica Peruana observata sunt. *Archiv für Naturgeschichte* 1847; 13:67–185.

Fabricius JC. *Systema Entomologiae, Sistens Insectorvm Classes, Ordines, Genera, Species, Adiectis Synonymis, Locis, Descriptionibvs, Observationibus*. Kortii, Flensburg and Leipzig ['Flensburgi et Lipsiae']: Havniae [= Copenhagen], 1775, [32] + 832.

Fabricius JC. *Species Insectorvm Exhibentes Eorvm Differentias Specificas, Synonyma Avctorvm, Loca Natalia, Metamorphosin Adiectis Observationibvs, Descriptionibvs*. Carol. Ernest. Bohn, Hambvrgi et Kilonii [= Hamburg & Kiel], Tom. I, 1781, viii + 552.

Fiori G. La cavita sottoelitrale dei tenebrionidi apomorfi. *Redia* 1977; 60:1–112.

Goloboff PA. Estimating character weights during tree search. *Cladistics* 1993; 9:83–91. https://doi.org/10.1111/j.1096-0031.1993.tb00209.x

Goloboff PA, Catalano SA. TNT version 1.5, including a full implementation of phylogenetic morphometrics. Cladistics 2016; 32:221–38. https://doi.org/10.1111/cla.12160

Goloboff PA, Farris J. Methods for quick consensus estimation. *Cladistics* 2001; 17:S26–34.

Goloboff PA, Farris JS, Källersjö M et al. Improvements to resampling measures of group support. *Cladistics* 2003; 19:324–32.

Goloboff PA, Carpenter JM, Arias JS et al. Weighting against homoplasy improves phylogenetic analysis of morphological data sets. *Cladistic*s 2008a; 24:758–73. https://doi.org/10.1111/j.1096-0031.2008.00209.x

Goloboff PA, Farris JS, Nixon KC. TNT, a free program for phylogenetic analysis. *Cladistics* 2008b; 24:774–86. https://doi.org/10.1111/j.1096-0031.2008.00217.x

Gómez RS. Trogidae. In: Claps LE, Debandi G, Roig-Juñent S (eds), *Biodiversidad de Artrópodos Argentinos II.* Buenos Aires: Sociedad Entomológica Argentina, 2008, 509–18.

Haaf E. Die Afrikanische arten der gattung *Trox. Entomologische Arbeiten aus dem Museum G. Frey* 1953; 4:309–46.

Haaf E. Eine neue *Trox*-art aus Süd-Afrika. *Durban Museum Novitates* 1954; 4:97–9.

Harold E. Monographie der Gattung *Trox. Coleopterologische Hefte* 1872; 9–10:1–192.

d'Hotman D, Scholtz CH. Phylogenetic significance of the structure of the external male genitalia in the Scarabaeoidea (Coleoptera). *Entomology Memoir Department of Agricultural Development* 1990; 77:1–51.

Huchet JB, Costa-Silva V. A new species of *Polynoncus* Burmeister, 1876 from Brazil (Coleoptera: Trogidae). *Zootaxa*, 2018; 4524:553–66. https://doi.org/10.11646/zootaxa.4524.5.3

Hughes J, Vogler AP. Gene expression in the gut of keratin-feeding clothes moths (Tineola) and keratin beetles (*Trox*) revealed by subtracted cDNA libraries. *Insect Biochemistry and Molecular Biology* 2006; 36:584–92. https://doi.org/10.1016/j.ibmb.2006.04.007

Iablokoff-Khnzorian SM. Über die Phylogenie der Lamellicornia (Insecta, Coleoptera). *Entomologische Abhandlungen / Staatlichen Museum für Tierkunde in Dresden* 1977; 41:135–200.

Kolbe HJ. Aufzählung der von Herrn Dr Hans Meyer im jahre 1889 im Gebiete des Kilimandscharo- und Ugueno-Gebirges gesammelten Coleopteren. *Stettiner Entomologische Zeitung* 1891; 52:18–36.

MacLeay WS. *Horae Entomologicae: or Essays on the Annulose Animals. Containing General Observations on the Geography, Manners, and Natural Affinities of the Insects which Compose the Genus Scarabaeus of Linnaeus; to Which are Added a few Incidental Remarks on the Genera Lucanus and Hister of the Same Author* [with an appendix and plates]. Vol. 1, Pt. 1. London: S. Bagster; 1819.

Martínez A, Pereira FA, Vulcano MA. Glaresini, nueva tribu de Trogidae para la región Neotropical. *Anales de la Sociedad Científica Argentina* 1961; 171:67–82.

McKenna DD, Shin S, Ahrens D et al. The evolution and genomic basis of beetle diversity. *Proceedings of the National Academy of Sciences* 2019; 116:24729–37.

Melsheimer FE. Descriptions of new species of Coleoptera of the United States. *Proceedings of the Academy of Natural Science of Philadelphia* 1846; 2:134–60.

Mirande JM. Weighted parsimony phylogeny of the family Characidae (Teleostei: Characiformes). *Cladistics* 2009; 25:1–40.

Nel A, Scholtz CH. Comparative morphology of the mouthparts of adult Scarabaeoidea (Coleoptera). *Entomology Memoir Department of Agricultural Development* 1990; 80:1–84.

Nikolajev GV. Omorgini (Coleoptera, Scarabaeidae, Troginae) – a new tribe of scarab beetles. *Euroasian Entomological Journal* 2005; 4:321–2 [in Russian].

Nikolajev GV. Taxonomic composition of the family Trogidae (Coleoptera: Scarabaeoidea) of the Russian fauna. *Caucasian Entomological Bulletin* 2016; 12:81–91 [in Russian].

Nixon KC. WinClada, v.1.00.08. 2002. http://www.cladistics.com. (19 July 2021, date last accessed).

O'Leary MA, Kaufman S. MorphoBank: phylophenomics in the 'cloud'. *Cladistics* 2011; 27:529–37. https://doi.org/10.1111/j.1096-0031.2011.00355.x

Olivier AG. Entomologie, ou histoire naturelle des insectes, avec leurs caractères génériques et spécifiques, leur description, leur synonymie, et leur figure enluminée. Coléoptères. In: *Tome Primier*. Paris: Baudouin, 1789, xx + 433.

Pittino R. New Coleoptera Trogidae from South America (XXXII contribution to the knowledge of Coleoptera Scarabaeoidea). *Giornale Italiano di Entomologia* 1987; 3:377–97.

Pretorius E, Scholtz CH. Geometric morphometrics and the analysis of higher taxa: a case study based on the metendosternite of the Scarabaeoidea (Coleoptera). *Biological Journal of the Linnean Society* 2001; 74:35–50. https://doi.org/10.1111/j.1095-8312.2001.tb01375.x

Robinson M. Studies in the Scarabaeidae II. *Transactions of the American Entomological Society* 1940; 66:141–60.

Robinson M. A new species of *Trox* from Texas. *Entomological News Philadelphia* 1941; 52:134–5.

Roff DA. The evolution of flightlessness in insects. *Ecological Monographs* 1990; 60:389–421. https://doi.org/10.2307/1943013

Scholtz CH. Aptery in Trox (Coleoptera: Trogidae): morphological changes and their relationship to habitat. *Journal of Entomological Society of Southern Africa* 1981; 44:83–7.

Scholtz CH. Phylogeny and systematics of the Trogidae (Coleoptera: Scarabaeoidea). *Systematic Entomology* 1986; 11:355–63. https://doi.org/10.1111/j.1365-3113.1986.tb00186.x

Scholtz CH. Phylogenetic trends in the Scarabaeoidea (Coleoptera). *Journal of Natural History* 1990a; 24:1027–66. https://doi.org/10.1080/00222939000770631

Scholtz CH. Revision of the Trogidae of South America (Coleoptera: Scarabaeoidea). *Journal of Natural History* 1990b; 24:1391–456. https://doi.org/10.1080/00222939000770841

Scholtz CH. Evolution of flightlessness in Scarabaeoidea (Insecta, Coleoptera). Mitteilungen aus dem Museum für Naturkunde in Berlin. *Deutsche Entomologische Zeitschrift* 2000; 47:5–28. https://doi.org/10.1002/mmnd.4800470102

Scholtz CH, Peck S. Description of a Polynoncus Burmeister larva, with implications for phylogeny of the Trogidae (Coleoptera: Scarabaeoidea). *Systematic Entomology* 1990; 15:383–9. https://doi.org/10.1111/j.1365-3113.1990.tb00072.x

Sereno PC. Logical basis for morphological characters in phylogenetics. *Cladistics* 2007; 23:565–87. https://doi.org/10.1111/j.1096-0031.2007.00161.x

Smith ABT, Hawks DC, Heraty JM. An overview of the classification and evolution of the major scarab beetle clades (Coleoptera: Scarabaeoidea) based on preliminary molecular analyses. *Coleopterists Society*, 2006, Monograph No. 5:35–46.

Strong EE, Lipscomb D. Character coding and inapplicable data. *Cladistics* 1999; 15:363–71. https://doi.org/10.1111/j.1096-0031.1999.tb00272.x

Strümpher WP, Sole CL, Villet MH et al. Phylogeny of the family Trogidae (Coleoptera: Scarabaeoidea) inferred from mitochondrial and nuclear ribosomal DNA sequence data. *Systematic Entomology* 2014; 39:548–62. https://doi.org/10.1111/syen.12074

Strümpher WP, Villet MH, Sole CL et al. Overview and revision of the extant genera and subgenera of Trogidae (Coleoptera: Scarabaeoidea). *Insect Systematics & Evolution* 2016; 47:53–82. https://doi.org/10.1163/1876312x-46052133

Vaurie PA. Revision of the genus Trox in South America (Coleoptera, Scarabaeidae). *Bulletin of the American Museum of Natural History* 1962; 124:101–67.

Wagner DL, Liebherr JK. Flightlessness in insects. *Trends in Ecology & Evolution* 1992; 7:216–20. https://doi.org/10.1016/0169-5347(92)90047-F

Zídek J. Updated checklist and bibliography of family Trogidae (Coleoptera: Scarabaeoidea). *Folia Heyrovskyana (Series A)* 2017; 25:93–127.